1964

The atomic absorption spectra of the lanthanide elements

Victor Giovoni Mossotti
Iowa State University

THE ATOMIC ABSORPTION SPECTRA OF THE LANTHANIDE ELEMENTS

by

Victor Giovoni Mossotti

A Dissertation Submitted to the
Graduate Faculty in Partial Fulfillment of
The Requirements for the Degree of
DOCTOR OF PHILOSOPHY

Major Subject: Physical Chemistry

Approved:

Signature was redacted for privacy.

In Charge of Major Work

Signature was redacted for privacy.

Head of Major Department

Signature was redacted for privacy.

Dean of Graduate College

Iowa State University
Of Science and Technology
Ames, Iowa

1964

TABLE OF CONTENTS

		Page
I.	INTRODUCTION	1
II.	MEASUREMENT OF SPECTRA	7
	A. Apparatus	7
	B. Photographic Recording of Spectra	18
	C. Observations	21
III.	IMPLICATIONS OF RESULTS	63
	A. The Role of the Free Atom	63
	B. A Possible Flame Mechanism	65
	C. Suggestions for Further Investigation	71
IV.	ANALYTICAL APPLICATIONS	76
	A. Preliminary Observations	76
	B. Instrumentation	87
	C. Results	102
	D. Conclusion	125
	E. Suggestions for Further Investigation	126
V.	SUMMARY	129
VI.	LITERATURE CITED	131
VII.	ACKNOWLEDGEMENTS	138

I. INTRODUCTION

There is presently a two fold interest in the atomic absorption spectra of the lanthanide elements. Since the absorption lines originate in the ground level, or in other low lying terms of the neutral atom or ion, many of the observed transitions should have lower energy levels in common. The wavelengths of the absorption lines, therefore, furnish a convenient starting point for unraveling the complicated energy level structure of these elements. Early workers found that atomic absorption spectra of many elements could be obtained by vaporizing salts in furnaces and by observing the sharp absorption lines against background continuum. Thus, Paul (1) used a modified King furnace charged with rare earth salts to observe the atomic absorption spectra of some of the elements in this group. In addition to 2500 lines reported for cerium, neodymium, and samarium, Paul has also indicated (2) that the absorption spectra have been observed for europium, dysprosium, holmium, thulium, and ytterbium, but their wavelengths have not been recorded in the literature. Bovey and Garton (3, 4) used a similar apparatus to observe 150 lines for thulium and lutetium. Recently, Sugar (5) described a pulsed arc

discharge producing highly self-reversed spectral lines for ytterbium, thulium, and terbium. This technique has served to determine the ground state configuration for Tb I and U II and to confirm those reported for Yb I, Yb II, Tm I, Tm II, and U I. Line reversal occurring in the spectra emitted by electrodeless discharge lamps containing metal iodides has been used by Worden, Gutmacher, and Conway (6) to determine the ground term level scheme for curium. The technique has been applied to other actinides and to most of the lanthanides, but no data have been published.

A second interest in these spectra arises from the increased application of atomic absorption to the determination of trace elements. Since Walsh (7) introduced the technique in 1955, approximately 200 papers describing the application of atomic absorption spectroscopy to practical analysis have appeared in the literature. In addition, fourteen extensive reviews (8-21) and one book (22) on atomic absorption analysis are available. The review by David (21) gives an exhaustive and recent coverage of all work in the field. In this technique, solutions of the samples are introduced as an aerosol into flames; thereby, free-atoms of many constituents in the sample are produced.

Unfortunately, formation of stable monoxide molecules by most of the lanthanides in stoichiometric flames reduces the free-atom population to such a degree that useful absorption cannot be observed. This deficiency in atomic absorption spectroscopy is not confined to the lanthanide elements; indeed, this situation prevailed in 1962 for about 28 elements. Metallic elements without useful atomic absorption lines in oxygen-hydrogen or in stoichiometric oxygen-acetylene flames are listed in Table 1. Naturally, the inability to detect so many important elements has greatly restricted the scope of application of atomic absorption.

In considering the basic difficulties presented by this group of elements, it is instructive to recall the closely related problem confronting the analytical flame spectroscopist. The conventional flame spectra of these same elements are found to be virtually devoid of lines, the most prominent feature being the metal oxide band systems (23).

Recent studies in our laboratory have revealed striking enhancements in the atomic spectra emitted by vanadium, titanium, niobium, rhenium, and the lanthanides when ethanolic solutions of their compounds are aspirated into fuel-rich oxygen-acetylene flames. The degree of enhancement

Table 1. Metallic elements without useful atomic absorption lines in oxygen-hydrogen or oxygen-acetylene flames

Scandium	Dysprosium	Niobium
Yttrium	Holmium	Zirconium
Lanthanum	Erbium	Hafnium
Cerium	Thulium	Thorium
Praseodymium	Ytterbium	Tantalum
Neodymium	Lutetium	Uranium
Samarium	Vanadium	Tungsten
Europium	Titanium	Osmium
Gadolinium	Rhenium	Iridium
Terbium		

is markedly affected by the choice of solvent. The flame spectra of dysprosium, as shown in Figure 1, provides a good example of this effect.

In previous publications (24, 25) these enhancements have been interpreted in terms of an environment (in the fuel-rich oxygen-acetylene flame) more conducive to the existence of free atoms of the lanthanides. If this interpretation is valid, the lanthanide atomic absorption spectra

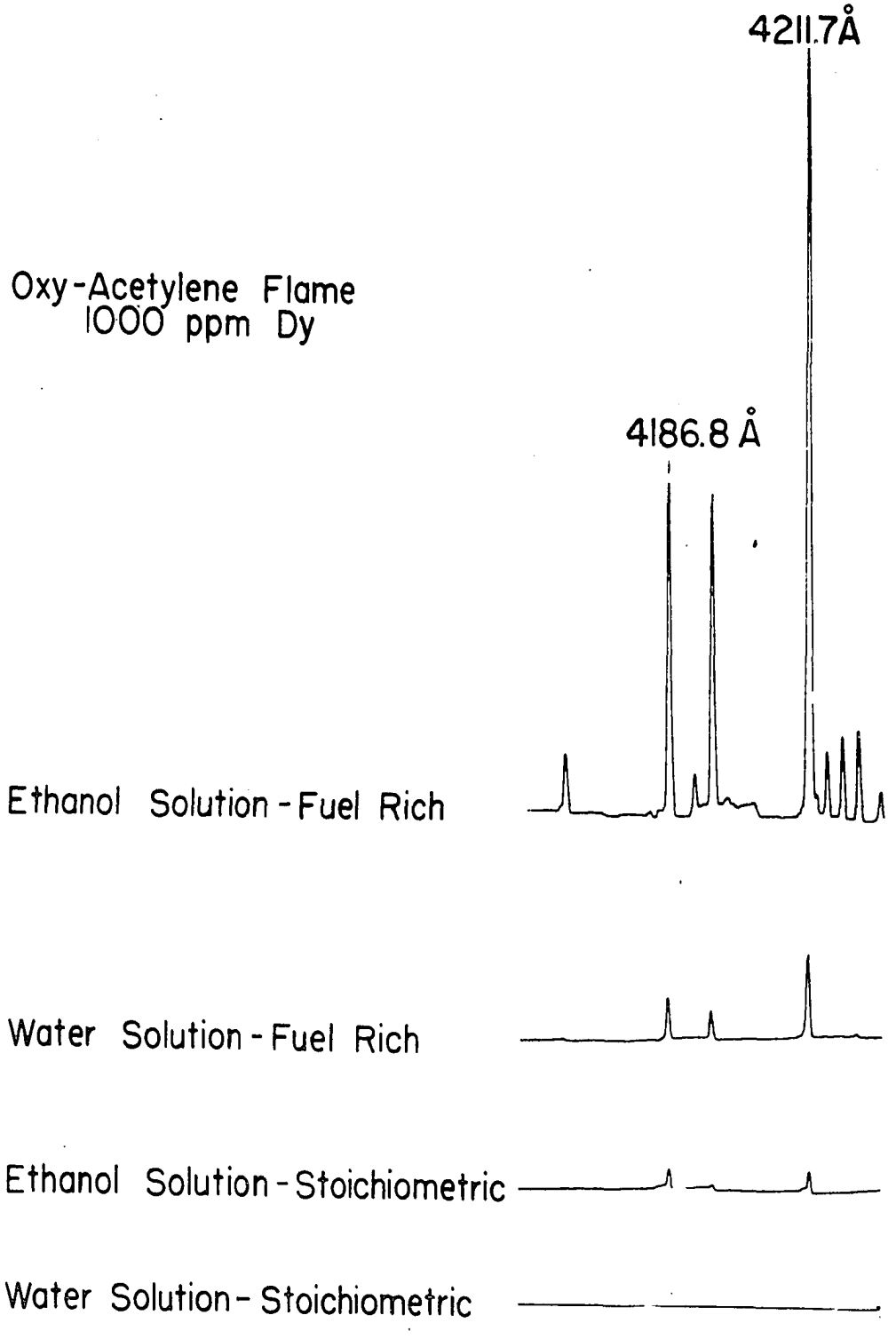

Figure 1. Effect of fuel and solvent on flame spectrum of dysprosium

should show a similar degree of enhancement. It is the purpose of this thesis to (a) provide experimental verification of the above interpretation and (b) to explore the analytical potentialities of the observed spectra.

II. MEASUREMENT OF SPECTRA

A. Apparatus

The experimental method of atomic absorption can be considered in four parts: source, atomic vapor, monochromator, and detector. In common practice a hollow-cathode lamp is used for the source. The line spectra emitted by the hollow-cathode in effect narrow the spectral band pass of the instrument. If a continuum is used the burden of narrowing the band pass falls entirely on the monochromator. The subject of sources will be considered in greater detail under analytical applications.

Although a flame is most often used to produce the atomic vapor, a variety of other techniques have been tried. Those that could be mentioned are hollow-cathode sputtering (26-29), the spark-in-spray approach (30), the King furnace method (31), a scheme which utilizes a discharge tube (32), and a capacitor discharge lamp method (33). A flame was used throughout this work.

The atomic absorption spectra reported in this section were observed photographically against a continuous background. This approach was selected for several reasons. It

provides a relatively simple and direct tool for exploring the effect of flame conditions on the free-atom population. In many instances the strongest atomic absorption lines do not correspond to the most sensitive lines in emission. It is necessary, therefore, to empirically determine the sensitive absorption lines. Moreover, with a continuum, it is possible to survey large portions of the spectrum without changing the source. In addition, this approach makes it easy to evaluate the feasibility of utilizing the atomic absorption spectra of the rare earths in an analytical method.

1. Burners and flames

Stationary flames may be considered to be of two general types. In the first, the properties of the flame are controlled by the rate of diffusion of the fuel into the ambient oxidant. This is popularly known as a diffusion flame. The familiar match flame provides an example of this type. In the second general type of stationary flame, the fuel and oxidant are intimately mixed before burning. In this case, the physical and chemical properties of the flame are largely governed by the kinetics of the combustion process. A good example of this type is the common Bunsen flame. A

stationary flame can be maintained at the top of the burner if the premixed gases flow up the burner tube at a rate which exceeds the normal burning velocity of the mixture. There is a conspicuous difference between the diffusion flame and premixed flame. For the latter, the kinetically controlled combustion process results in a well defined flame front and reaction zone. A flame of this variety will be considered further in the analytical application section. The flame produced by a diffusion process usually exhibits no distinct zones. Flames of this sort do not lend themselves to theoretical treatment; consequently, they have not been studied extensively.

Except for one experiment described later, the turbulent diffusion flame produced by a Beckman integral-aspirator burner (#4030) was used throughout this work. The schematic diagram shown in Figure 2 illustrates the main features of this burner. The direct dependence of solution aspiration on the oxygen flow rate is the major disadvantage of this design. This disadvantage may be circumvented through the use of a commercial infusion pump.

For most experiments it was found advantageous to use three flames to increase the path length through the atomic

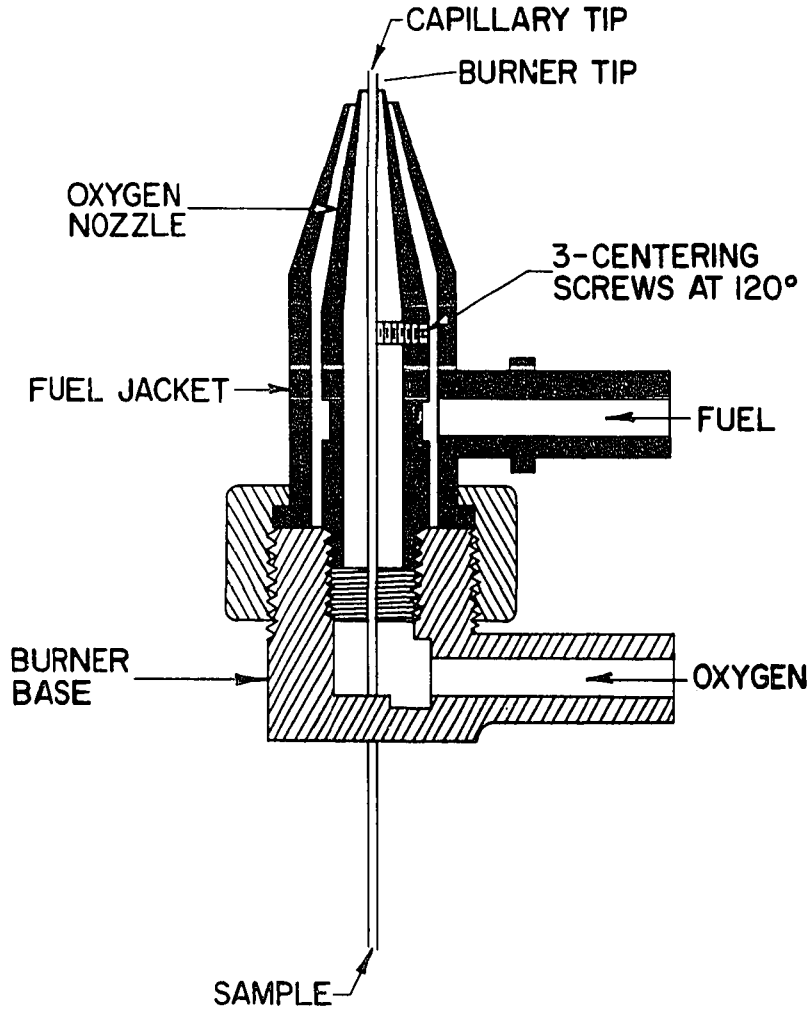

Figure 2. Beckman integral-aspirator burner

vapor. The construction and design of a highly functional triple burner mounting is shown in Figure 3. The mounting was designed around the framework of a microscope mechanical stage (Lafayette Radio Electronics #F-613). The solution was conveyed to the burner capillaries through one foot lengths of polyethylene tubing (Aloe Scientific #PE60).

2. Gas handling system

The gas handling system shown in Figure 4 was designed to continuously monitor the oxygen and acetylene flow rates. Low flow gas regulators (Mason-Neilan model 113) with a working pressure range of 2-20 psig. maintained a constant pressure in each system. High accuracy rotameters (Brooks Instrument Co. model FV1110), 600 mm in length, and having ±1 percent instantaneous accuracy, and better than 1/4 percent reproducibility, were used as flow rate measuring devices. The rotameters were factory calibrated for flow rates in the range 1.6 to 16 liters/minute at 10 and 5 psig. for oxygen and acetylene respectively. Correction curves also were provided for a full range of working pressures. Variable orifices consisting of low taper needle valves (Ideal Aerosmith #51-4-23) provided throttling control for oxygen and acetylene flow. The pressure of each system was

Figure 4. Gas flow metering system

continuously monitored (Marshalltown pressure gauges, 3 1/2 inch dial faces, 0-30 psig.). The entire system was panel mounted in a portable forty inch wooden cabinet. The inlet and outlet connections were Swagelok bulkhead quick-connects (Swagelok #400-QC-61). This feature made it possible to transport the equipment from one flame facility to another with a minimum amount of time and effort.

A gas manifold system downstream from the rotameter provided precise control of the gas flow to the tandem burner set. This consisted of toggle and regulating valves (Hoke, Series 450) all conveniently panel mounted in a six inch metal box.

3. Source

The background continuum for the 2500-4300 Å region was obtained from a 150 watt high pressure xenon arc (Hanovia Chemical and Mfg. Co., #2931). Radiations from xenon discharges are often compared to those of black body radiators at temperatures of 6000 to 7000 ^{o}K (34-36). The comparison is usually valid only for the visible part of the spectrum. The continuum from a 500 watt tungsten filament lamp was used to extend the observations up to 6500 Å.

4. External optics

As reported by a number of authors (37, 38), atomic emission and absorption spectra resulting from elements having a tendency to form stable molecular species in the flame are very sensitive to variations in height along the flame axis. Probing experiments in which lanthanide atomic absorption measurements were made at different heights in the flame confirm this expected behavior. A multiple pass optical system was designed with this observation in mind. The optical elements consisted of a Jarrell-Ash #82330 multiple pass attachment modified so that three traversals of the xenon continuum passed through the portion of the flame exhibiting maximal absorption. The modifications made in the Jarrell-Ash attachment were as follows: As is apparent in Figure 5, the mirrors and lenses in the modified attachment were mounted in the horizontal plane. The three flames were situated centrally between the mirror-lens assemblies. Continuous radiation from the off-axis xenon arc was focused on the central flame by the source lens. The light traversed all three flames at a distance 25 mm above the burner tip. The transmitted radiation was then reflected by mirror A to mirror B. After reflection at

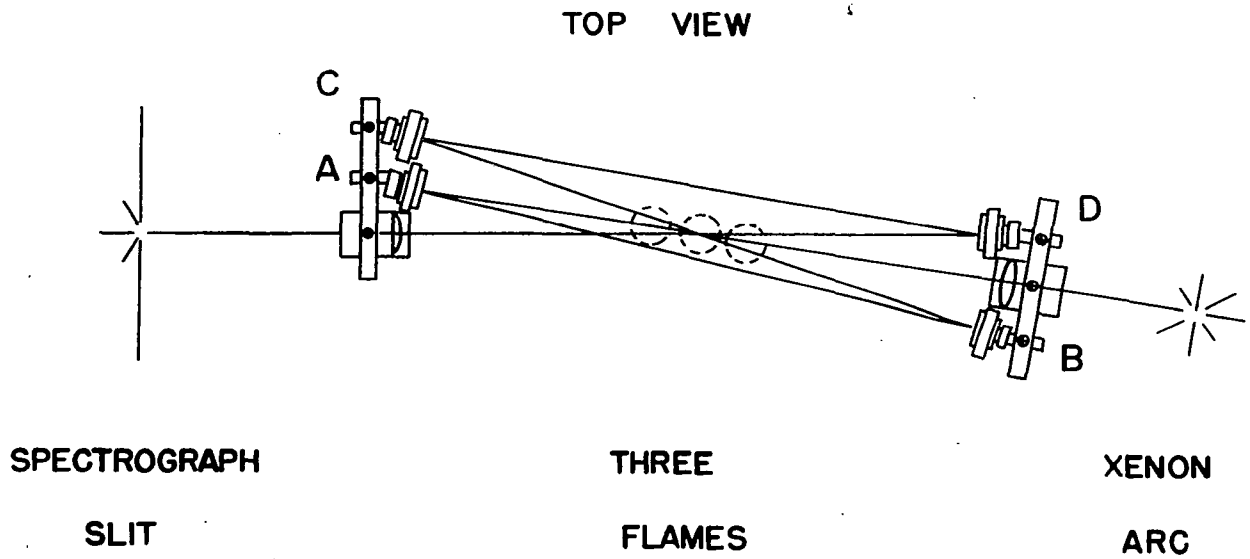

Figure 5. Multipass optical system for photographic recording of atomic absorption spectra

mirror B, the light again passed through all three flames at the optimum distance above the burner tip; the transmitted light was then reflected by mirror C to mirror D. The latter formed an image of the source on the central flame 25 mm above the burner tip.

A conventional crossed cylindrical lens system was employed to form an image of the xenon source on the collimating mirror of the spectrograph (39).

B. Photographic Recording of Spectra

1. Fuel ratio

Assuming the combustion mixture expands to atmospheric pressure before burning, the volume flow rates are proportional to the molar flow rates. If complete combustion to carbon monoxide and water is assumed the oxygen/acetylene molar ratio would be 1.5 for a stoichiometric flame.

To establish the optimum flame conditions, absorption profiles were determined for various oxygen/fuel ratios. To insure a constant sample aspiration rate the oxygen flow rate was fixed at 2.68 l/min through each burner. The fuel then could be varied independently.

Maximal atomic absorption spectra were observed when the

flame was operated under highly fuel-rich conditions. The oxygen and acetylene flow rates were 2.68 l/min and 3.16 l/min respectively.

2. Burner matching

The procedure for matching gas flow rates through each burner was relatively simple. Since the burners were arranged in parallel it was possible to set the gas flow through each burner separately. That is, with two of the burners clamped off the gas flow through one burner was set at the desired value. The procedure was repeated until the needle valves for all three burners for both oxygen and acetylene were correctly set for a given flow rate at the desired pressure of the system.

The rate at which solution was consumed from a small graduate cylinder gave a measure of the sample aspiration rate for each burner. Typical values ranged from 0.6 to 0.9 ml/min.; the rate depended on the individual burner. It should be noted, however, that these values showed little variation with extended use of the burner. Changes in the aspiration rate were usually sudden; these resulted from a clogged burner or misaligned capillary. Such changes were usually reflected by the physical appearance and audibility

of the flame.

3. Solutions

The observations reported in Table 3 were made on one percent ethanolic solutions of perchlorate salts of the elements. All solutions used in these experiments were prepared in accordance with the procedures described previously (24, 40).

4. Photographic conditions

The atomic absorption spectra were photographed in juxtaposition with an iron arc reference spectrum. Wavelengths were measured by interpolation between iron lines. More exact wavelengths were assigned by reference to the M. I. T. Wavelength Tables (41) or the NBS Tables of Spectral Line Intensities (42). The spectra were photographed under the experimental conditions summarized in Table 2.

Table 2. Experimental conditions for photographic recording of absorption spectra

Spectrograph	Jarrell-Ash Co., 3.4 meter mounting plane grating spectrograph, using 6-inch, 15,000 lines/inch grating blazed for 5000 Å, first order
Order	First
Reciprocal linear dispersion	5.2 Å/mm
Wavelength regions on photographic emulsions	2400-6500 Å Spectrum Analysis #1, KM
Exposure time	8 seconds
Sector	All exposures were made through a rotating eight-step sector
Slit height	10 mm
Slit width	0.010 mm
Height in flame	25 ± 5 mm
Gas flow rates	Oxygen: 2.68 l/min Acetylene: 3.16 l/min

C. Observations

In view of the arguments presented in the introduction, it is reasonable to expect that atomic absorption enhancements afforded by the fuel-rich flame--if any--should be

influenced by the dissociation energy of the metal oxide. Indeed, a striking trend can be seen in Figures 6 and 7. Each pair of spectrograms shown in the figures is comprised of a fuel-rich flame absorption spectrogram in juxtaposition below a stoichiometric flame spectrogram.

Referring to the figures, one can see that the stability of thulium monoxide is low enough for appreciable free atom concentrations in a stoichiometric flame.

Dysprosium is barely detectable in the stoichiometric flame; the strong tendency for monoxide formation is reflected by the higher dissociation energy. Again, the enhancement is remarkable in the fuel-rich flame.

Since vanadium monoxide is more stable, absorption lines are barely visible in the upper spectrogram. There are, however, strong vanadium lines in the fuel-rich flame spectrum.

Although titanium lines are not detectable in the stoichiometric flame spectrogram, they are readily apparent in the fuel-rich flame spectrogram. It is worth noting that manganese oxide is not a particularly stable molecule; clearly, the stoichiometric and fuel-rich flames are equally populated with free manganese atoms. The manganese lines

Figure 6. Effect of oxygen/fuel ratio on flame absorption spectra of thulium and dysprosium

DYSPROSIUM
D_o^o = 6.2 eV (est.)
4186.81
4191.63
4194.83
4211.72
4213.18
4215.15
4218.09
4221.10
4225.14
4226.73 Ca I

THULIUM
D_o^o = 5.0 (est.)
3717.92
3744.07
3751.82

Figure 7. Effect of oxygen/fuel ratio on flame absorption spectra of vanadium and titanium

TITANIUM
D_o^o = 6.9 eV
3981.76
3989.76
3998.64
4008.93
4024.57
4030.76 Mn
4033.07 Mn
4034.49 Mn
VANADIUM
D_o^o = 6.4 eV
3183.41
3183.98
3185.40
3198.12
3202.38
3207.41

provide convincing evidence that the over-all instrumental sensitivity remained unchanged throughout the experiment.

A similar effect of oxygen/fuel ratio on absorption has been observed for rhenium, niobium, the remaining lanthanides, and a host of common elements. A further report on the analytical application of these results will be given later.

Table 3 lists the observed wavelengths, relative degree of absorption, spectral classifications, and energy combinations where known for more than 1000 lines. Except for cerium, which remains undetected by this method, the spectra of all members of the lanthanide series as well as the spectra of vanadium, titanium, and niobium are reported. The lines in Table 3 represent the first reported observations of atomic absorption spectra of these elements in flames. Until now the atomic absorption spectra of erbium and gadolinium had never been reported by any technique. Also, the wavelengths listed in Table 3 for europium, dysprosium, praseodymium, holmium, and terbium are the first to appear in the literature (43). All of the lines observed by the author are included in Table 3 so as to make the table a self contained entity. The lines previously reported by Paul (1, 2) and Bovey and Garton (3, 4) are appropriately identified.

Each line has been assigned to one of five intensity categories in accordance with the observed degree of absorption. A visually very weak line is denoted (VW), whereas a line having enough intensity to be easily detected against the continuous background but of no analytical importance is designated (W). Lines exhibiting adequate sensitivity to show analytical promise are denoted medium (M), strong (S), and very strong (VS).

The energy levels involved in the absorption transitions have been assigned for some of the lines in Table 3. These assignments are tabulated in the fourth column. Examination of these data reveals that all of the known transitions originate in the ground state terms of either the parent atom or its ion. It is reasonable to conclude, therefore, that the same origin can be expected for those lines having no energy level assignments. In view of the common origin of the lines in Table 3, the wavelengths should be of value in deducing the low lying energy level structure of those rare earth systems which are still not analyzed.

Table 3. Atomic absorption spectra of the rare earth elements (and vanadium, titanium, and niobium)

Wavelength[a] (Å)	Relative[b] Intensity	Spectrum[c]	Energy levels[d] (cm^{-1})
		Lanthanum	
3574.43	M	I	0-27969
3927.56	W	I	0-25454
4015.39	VW	I	1053-25950
4037.21	W	I	0-24763
4079.18	VW	I	0-24508
		Praseodymium	
3908.43	VW	II	
4635.69	VW	I	
4639.56	VW	I	
4730.69	VW	I	

[a]Measured wavelengths are corrected to values given in the NBS "Tables of Spectral-Line Intensities" (42) except those marked by * which denotes wavelength corrected to value given in MIT Wavelength Tables (41) or by ** which denotes a line for which no corresponding wavelength was found in either of the above works. In this case the wavelength is given to the nearest 0.1 Å as measured by the author.

[b]VS-Very Strong
S-Strong
M-Medium
W-Weak
VW-Very Weak

[c]I indicates neutral atom line; II denotes ion lines; N indicates no data available.

[d]Energy level data and spectrum assignments were taken from NBS "Tables of Spectral-Line Intensities" (42).

Table 3 (Continued)

Wavelength[a] (Å)	Relative[b] Intensity	Spectrum[c]	Energy levels[d] (cm^{-1})
	Praseodymium (Continued)		
4736.69	W	I	
4744.16	VW	I	
4914.03	W	I	
4924.59	W	I	
4939.74	W	I	
4940.30	W	I	
4951.36	M	I	
4976.40	VW	I	
5018.58	W	I	
5019.76	W	I	
5026.97	W	I	
5033.38	W	I	
5043.83	W	I	
5045.53	M	I	
5053.40	W	I	
5087.11	VW	I	
5133.42	M	I	
5139.80	VW	I	
5194.41	VW	I	
5228.01	VW	I	
	Neodymium[e]		
3346.59*+	W	I	
3358.72*+	W	I	
3721.35	VW	II	
3787.52*	VW	I	
3793.64*+	VW	I	
3830.92*+	VW	I	
3887.87	VW	II	513-26227

[e]Lines marked + have been reported by Paul (1, 2).

Table 3 (Continued)

Wavelength[a] (Å)	Relative[b] Intensity	Spectrum[c]	Energy levels[d] (cm^{-1})
	Neodymium (Continued)		
3935.92*+	VW	I	
4256.47+	W	I	
4343.50+	VW	I	0-23016
4444.99+	W	I	0-22491
4456.13*+	VW	I	
4477.88+	VW	I	
4480.97+	W	I	1128-23438
4481.90+	W	I	1128-23434
4529.94	VW	I	
4542.06+	W	I	0-22010
4559.67+	W	I	2367-24292
4560.42+	W	I	
4586.62+	VW	I	
4594.45+	VW	II	1650-23410
4609.87+	W	I	1128-22815
4621.94+	W	I	2367-23996
4624.21+	VW	I	
4626.50+	VW	I	1128-22737
4627.98+	VW	I	2367-23968
4634.24+	M	I	0-21572
4637.20+	VW	I	0-21559
4639.14+	W	I	1128-22678
4641.10+	W	I	
4646.40+	W	I	
4649.67+	W	I	
4651.02*+	VW	I	
4652.39+	W	I	
4654.73+	W	I	1128-22606
4683.45+	M	I	0-21346
4684.04+	W	I	1128-22471
4690.35+	M	I	0-21314
4696.44+	VW	I	3682-24968
4706.96+	M	I	1128-22367
4719.02+	M	I	
4731.78+	W	I	1128-22256

Table 3 (Continued)

Wavelength[a] (Å)	Relative[b] Intensity	Spectrum[c]	Energy levels[d] (cm^{-1})
	Neodymium (Continued)		
4749.75+	VW	I	3682-24730
4770.20+	VW	I	
4772.26+	VW	I	
4779.46+	W	I	
4806.62+	VW	I	1128-21927
4835.66+	VW	I	2367-23040
4836.62+	W	I	
4853.33+	VW	I	1128-21727
4855.31+	VW	I	1128-21718
4859.58+	VW	I	
4866.74+	W	I	0-20542
4879.79+	VW		
4883.81+	M	I	
4891.07+	M	I	
4893.23+	W	I	1128-21559
4896.93+	M	I	1128-21543
4901.53+	W	I	
4901.84+	M	I	
4907.26+	VW	I	2367-22739
4907.78+	VW	I	2367-22737
4910.05+	W	I	0-20361
4913.41+	M	I	
4924.53+	S	I	0-20301
4944.83+	M	I	
4952.46+	W	I	1128-21314
5029.45+	VW	I	1128-21005
5056.89+	W	I	0-19770
5103.11+	VW	I	
5105.35+	VW	I	
5149.56*+	VW	I	
5198.07+	VW	I	1128-20361
5199.73*+	VW	I	
5204.38+	VW	I	0-19209
5561.17+	VW	I	0-17977
5620.54+	M	I	0-17787

Table 3 (Continued)

Wavelength[a] (Å)	Relative[b] Intensity	Spectrum[c]	Energy levels[d] (cm^{-1})
	Neodymium (Continued)		
5675.97+	W	I	1128-18741
5729.29+	VW	I	
	Samarium		
3586.36*	VW	I	
3592.60+	VW	II	3053-30880
3604.28+	VW	II	3910-31646
3607.64*+	VW	I	
3609.49+	VW	II	2238-29935
3629.22*+	W	II	
3634.29+	VW	II	1489-28997
3651.52*+	VW	I	
3657.32*+	W	I	
3661.36+	VW	II	327-27631
3666.27*+	VW	I	
3670.84+	VW	II	838-28073
3687.88*+	W	N	
3690.08+	W	I	2273-29365
3706.98+	W	II	
3707.63*+	W	I	
3721.03+	W	I	1490-28356
3722.02*+	W	I	
3728.16*+	VW	I	
3730.74+	VW	I	2273-29070
3731.26	VW	II	838-27631
3737.14+	VW	II	
3739.20+	W	II	327-27063
3745.46+	M	I	1490-28181
3748.52+	M	I	293-26962
3756.41+	M	I	812-27426
		II	3499-30113
3760.05+	W	II	3053-29641
3773.33+	M	I	
3782.68+	W	I	

Table 3 (Continued)

Wavelength[a] (Å)	Relative[b] Intensity	Spectrum[c]	Energy levels[d] (cm^{-1})
		Samarium (Continued)	
3803.94+	M	I	0-26281
3809.88+	W	II	838-27078
3813.83+	W	I	4021-30234
3818.36+	VW	I	1490-27671
3822.96*+	W	I	
3832.81+	W	I	2273-28356
3834.48+	M	I	4021-30093
3846.28+	W	I	
3846.76+	VW	I	293-26281
3848.78	W	II	
3853.30+	W	I	3125-29070
3854.56+	W	I	1490-27426
3858.52+	W	I	1490-27399
3858.74+	W	I	2273-28181
3860.14*+	W	N	
3877.49+	W	I	4021-29803
3881.79	W	II	
3925.22+	M	I	812-26281
3951.89+	M	I	
3962.13+	W	I	
3974.66+	M	I	2273-27426
3978.24*+	VW	I	
3990.00+	M	II	0-25056
3991.02+	W	I	
3998.35+	W	I	
4062.32*+	VW	N	
4079.83+	W	I	2273-26777
4183.33+	W	I	1490-25387
4205.78+	W	I	
4226.18+	W	I	812-24467
4266.31+	VW	I	812-24245
4271.86+	VW	I	2273-25676
4282.21+	W	I	3125-26471
4282.83+	W	I	2273-25616
4283.50+	W	I	812-24151

Table 3 (Continued)

Wavelength[a] (Å)	Relative[b] Intensity	Spectrum[c]	Energy levels[d] (cm^{-1})
	Samarium (Continued)		
4296.74+	M	I	4021-27288
4299.14+	VW	I	293-23547
4312.85+	VW	I	2273-25453
4319.53+	W	I	1490-24634
4324.46+	VW	I	2273-25391
4330.02+	W	I	293-23381
4331.45+	W	I	
4336.14+	W	I	3125-26182
4338.96+	VW	I	812-23852
4339.92+	VW	I	812-23847
4362.91+	W	I	0-22914
4380.42+	W	I	1490-24312
4386.22+	VW	I	2273-25065
4393.35+	VW	I	1490-24245
4397.34+	W	I	812-23547
4401.17+	W	I	3125-25840
4403.13+	W	I	2273-24978
4411.58+	W	I	1490-24151
4419.33+	W	I	293-22914
4423.38+	VW	I	293-22893
4429.66+	W	I	812-23381
4433.08+	VW	I	293-22844
4441.81+	W	I	1490-23997
4442.28+	W	I	812-23317
4445.15+	W	I	3125-25616
4452.95+	W	I	4021-26471
4459.29+	W	I	812-23231
4470.89+	W	I	2273-24634
4480.32+	W	I	0-22314
4499.11+	W	I	1490-23710
4503.38+	W	I	293-22492
4511.33+	VW	I	4021-26182
4522.55+	VW	I	1490-23595
4523.18+	VW	I	812-22914
4527.42+	VW	I	812-22893
4532.44+	VW	I	1490-23547

Table 3 (Continued)

Wavelength[a] (Å)	Relative[b] Intensity	Spectrum[c]	Energy levels[d] (cm^{-1})
	Samarium (Continued)		
4533.80+	VW	I	2273-24324
4566.77+	VW	I	1490-23381
4569.58+	VW	I	2273-24151
4581.58+	M	I	812-22632
4596.74+	W	I	
4611.25+	VW	I	812-22492
4645.40+	W	I	293-21813
4648.16+	VW	II	0-21508
4649.49+	W	I	812-22314
4663.56+	W	I	2273-23710
4670.75+	W	I	1490-22894
4681.55+	W	I	1490-22844
4688.73+	W	I	2273-23595
4716.10+	W	I	3125-24324
4717.07+	W	I	0-21194
4718.64+	VW	I	3125-24312
4728.42+	M	I	1490-22632
4750.72+	VW	I	2273-23317
4760.27+	M	I	812-21813
4770.20+	VW	I	2273-23231
4783.10+	M	I	293-21194
4785.86+	M	I	812-21701
4789.96+	VW	I	3125-23997
4841.70+	W	I	4021-24669
4848.32+	W	I	2273-22893
4883.77+	W	I	293-20763
4883.97+	M	I	3125-23595
4904.97+	W	I	812-21194
4910.40+	W	I	2273-22632
4918.99+	W	I	1490-21813
4924.04+	VW	I	4021-24324
4946.32+	VW	I	1490-21701
4975.98+	W	I	0-20091
5044.28+	W	I	1490-21308
5071.20+	W	I	

Table 3 (Continued)

Wavelength[a] (Å)	Relative[b] Intensity	Spectrum[c]	Energy levels[d] (cm^{-1})
		Samarium (Continued)	
5088.32+	VW	I	812-20459
5117.16+	M	I	
5122.14+	M	I	3125-22643
5172.74+	W	I	2273-21600
5175.42+	M	I	
5200.59+	M	I	1490-20713
5251.92+	W	I	2273-21308
5271.40+	M	I	812-19777
5282.91+	M	I	1490-20413
5320.60+	VW	I	2273-21063
5341.29+	VW	I	293-19010
5368.36+	VW	I	4021-22643
5403.70+	VW	I	1490-19990
5405.23+	W	I	293-18788
5453.00+	VW	I	3125-21459
5466.72+	VW	I	1490-19777
5485.42+	VW	I	0-18225
5493.72+	W	I	812-19010
5498.21+	VW	I	293-18475
5511.09+	VW	I	2273-20413
5512.10+	VW	I	812-18949
5516.09+	W	I	2273-20397
5548.95+	VW	I	
5550.40+	VW	I	1490-19501
5621.79+	VW	I	293-18076
5626.01+	VW	I	0-17770
5659.86+	VW	I	812-18475
5706.20+	VW	I	1490-19010
5706.75+	VW		
		Europium	
3058.98	W	I	0-32681
3106.18	M	I	0-32185
3111.43	S	I	0-32130

Table 3 (Continued)

Wavelength[a] (Å)	Relative[b] Intensity	Spectrum[c]	Energy levels[d] (cm^{-1})
		Europium (Continued)	
3210.57	M	I	0-31138
3212.81	S	I	0-31116
3213.75	M	I	0-31107
3235.13	W	I	0-30902
3241.40	M	I	0-30842
3246.03	W	I	0-30798
3322.26	M	I	0-30091
3334.33	S	I	0-29982
3350.40	W	I	0-29839
3353.70*	W	I	
3432.52*	VW	I	
3457.05	W	I	0-28918
3467.88	W	I	0-28828
3589.27	W	I	0-27853
3688.42	W	II	0-27104
3724.94	M	II	0-26839
3819.67	S	II	0-26173
3907.10	W	II	1669-27256
3930.48	W	II	1669-27104
3971.96	W	II	1669-26838
4129.70	M	II	0-24208
4205.05	M	II	0-23774
4435.56	W	II	1669-24208
4522.57	VW	II	1669-23774
4594.03	VS	I	0-21761
4627.22	VS	I	0-21605
4661.88	VS	I	0-21445
5645.80	W	I	0-17707
5765.20	W	I	0-17341
6018.15	W	I	0-16612
		Gadolinium	
3604.87	VW	I	1719-29451
3674.05	VW	I	215-27425

Table 3 (Continued)

Wavelength[a] (Å)	Relative[b] Intensity	Spectrum[c]	Energy levels[d] (cm^{-1})
	Gadolinium (Continued)		
3684.13	W	I	0-27136
3713.57	W	I	215-27136
3717.48	W	I	533-27425
3732.32	VW	I	1719-28504
3732.67	VW	I	533-27316
3739.76	VW	I	999-27731
3744.83	VW	I	1719-28415
3757.94	VW	I	533-27136
3762.20	VW	I	999-27572
3783.05	W	I	999-27425
3843.28	VW	I	1719-27731
3866.99	VW	I	1719-27572
3934.79	VW	I	533-25940
3945.54	VW	I	999-26337
3969.00	VW	I	215-25403
4023.35	VW	I	533-25381
4045.01	VW	I	0-24715
4053.64	W	I	999-25661
4054.72	VW	I	0-24656
4058.22	W	I	215-24850
4078.70	W	I	533-25044
4090.41	VW	I	215-24656
4092.71	VW	I	1719-26146
4100.26	VW	I	999-25381
4175.54	VW	I	1719-25661
4190.78	W	I	999-24854
4191.63	VW	I	999-24850
4225.85	VW	I	1719-25376
4325.69	VW	I	533-23644
4327.12	VW	I	0-23104
		II	2857-25960
4346.46	VW	I	999-24000
4346.62	VW	I	215-23215
4422.41	VW	I	215-22821
4430.63	VW	I	0-22564

Table 3 (Continued)

Wavelength[a] (Å)	Relative[b] Intensity	Spectrum[c]	Energy levels[d] (cm^{-1})
		Terbium	
3494.93	W	I	
3516.64	W	I	
3518.96	VW	I	
3598.96*	VW	I	
3638.95	W	I	
3645.38	W	II	
3669.62	W	I	
3687.15*	VW	I	
3693.56	W	I	
3700.12	W	I	
3701.14	VW	I	
3701.33	VW	I	
3703.07	W	I	
3705.06	W	I	
3708.45	VW	I	
3711.74	VW	II	
3731.51	VW	I	
3743.65	VW	I	
3745.07	W	I	
3759.35	VW	I	
3760.13	W	N	
3761.12	VW	I	
3765.14	VW	I	
3769.43	VW	I	
3783.54	W	N	
3789.92	W	N	
3796.20	VW	N	
3804.42	VW	N	
3830.29	M	II	
3833.40	W	I	
3834.02	W	I	
3885.10	VW	I	
3888.23	VW	I	
3894.60	W	I	
3901.35	M	I	

Table 3 (Continued)

Wavelength[a] (Å)	Relative[b] Intensity	Spectrum[c]	Energy levels[d] (cm^{-1})
		Terbium (Continued)	
3908.08	W	I	
3915.43	M	I	
3932.37	VW	I	
3937.64	VW	I	
3942.95	VW	I	
3943.68	VW	I	
3950.14	VW	I	
3950.44	VW	I	
3951.88	VW	I	
3957.35	VW	I	
3962.61	VW	I	
4010.06	VW	I	
4010.85	VW	I	
4022.89	VW	I	
4023.72*	VW	I	
4024.79	VW	I	
4032.34	VW	I	
4038.86	VW	I	
4039.48	VW	I	
4047.14	VW	I	
4054.12	W	I	
4060.40	W	I	
4061.59	M	I	
4070.13	VW	I	
4071.22	VW	I	
4081.24	VW	I	
4086.62	VW	I	
4092.20	VW	I	
4094.05	VW	I	
4103.46	VW	I	
4105.37	M	I	
4112.50	W	I	
4112.88	VW	I	
4119.96	VW	I	
4130.14	VW	I	

Table 3 (Continued)

Wavelength[a] (Å)	Relative[b] Intensity	Spectrum[c]	Energy levels[d] (cm^{-1})
	Terbium (Continued)		
4132.48	VW	I	
4135.37	VW	I	
4139.06	VW	I	
4139.79	VW	I	
4141.55	VW	I	
4143.53	VW	I	
4146.96	VW	I	
4158.53	W	I	
4169.11	VW	I	
4169.31	VW	I	
4172.60	VW	I	
4172.82	VW	I	
4187.16	W	I	
4188.09	VW	I	
4196.73	W	I	
4203.72	W	I	
4206.49	VW	I	
4213.50	VW	I	
4215.13	W	I	
4217.56	VW	I	
4219.17	VW	I	
4224.28	VW	I	
4231.89	VW	I	
4232.82	VW	I	
4235.35	W	I	
4255.25	VW	I	
4258.23	VW	I	
4263.66	VW	I	
4266.34	W	I	
4298.37	VW	I	
4307.21	VW	I	
4310.44	VW	I	
4318.85	S	I	
4326.47	S	I	
4336.50	W	I	
4338.45	S	I	

Table 3 (Continued)

Wavelength[a] (Å)	Relative[b] Intensity	Spectrum[c]	Energy levels[d] (cm^{-1})
		Terbium (Continued)	
4340.62	M	I	
4356.84	W	I	
4423.11	W	I	
4493.08	W	I	
		Dysprosium	
2585.30	W	I	
2623.70	M	I	
2642.16	W	I	
2668.07	W	I	
2964.63	M	I	
2991.35	W	II	
2996.76*	W	I	
3001.03*	W	I	
3385.03	VW	II	
3393.59	VW	II	828-30287
3402.00	VW	II	
3407.79	W	II	0-29336
3434.37	VW	II	0-29109
3445.58	VW	II	0-29014
3454.35	VW	II	
3460.97	VW	II	0-28885
3494.49	VW	II	828-29437
3511.00*	W	I	
3515.64*	VW	I	
3521.13	VW	II	
3531.70	M	II	0-28307
3534.05*	VW	II	
3536.03	VW	II	
3538.50	W	II	0-28252
3547.89	VW	N	
3571.34	W	I	
3585.08	VW	II	0-27886
3594.57	W	N	

Table 3 (Continued)

Wavelength[a] (Å)	Relative[b] Intensity	Spectrum[c]	Energy levels[d] (cm^{-1})
	Dysprosium (Continued)		
3610.77*	VW	I	
3611.15	VW	I	
3643.50*	VW	I	
3645.41	W	II	828-28252
3646.85	VW	I	
3664.96*	VW	I	
3666.85	W	I	
3674.45	VW	II	
3678.48	W	I	
3685.81	M	I	
3694.81	VW	II	828-27886
3707.57	VW	II	
3727.99	VW	I	
3739.33	M	I	
3740.07*	M	I	
3741.18*	VW	I	
3757.05	M	I	
3767.63	M	I	
3771.08	M	I	
3772.65	VW	I	
3773.05	W	I	
3774.75	W	I	
3781.48	W	I	
3786.21	VW	II	
3788.46	W	II	828-27217
3797.76*	VW	I	
3809.95	W	N	
3812.30	W	I	
3816.21	VW	N	
3817.49	VW	N	
3819.44	VW	N	
3821.49	VW	N	
3821.85	VW	N	
3825.65	W	II	
3840.44*	VW	I	

Table 3 (Continued)

Wavelength[a] (Å)	Relative[b] Intensity	Spectrum[c]	Energy levels[d] (cm^{-1})
	Dysprosium (Continued)		
3840.91	W	I	
3844.30	W	I	
3846.99	W	I	
3858.41	W	I	
3868.81	M	I	
3872.13	W	II	0-25818
3874.00	VW	II	828-26634
3891.98*	W	I	
3892.87	W	I	
3898.54	VW	II	4756-30399
3899.15	VW	I	
3905.95	VW	I	
3913.62	W	I	
3917.30	W	I	
3930.15	VW	I	
3936.71	VW	I	
3937.16	VW	I	
3938.06*	VW	I	
3938.21*	VW	I	
3944.70	W	II	0-25343
3956.24	VW	I	
3962.58	VW	I	
3967.50	W	I	
3968.42	W	II	0-25192
3973.87	VW	I	
3981.37	VW	I	
3993.60	VW	I	
3994.53	VW	I	
3996.70	VW	II	4756-29769
3998.94*	VW	I	
4000.48	VW	II	828-25818
4005.86	W	I	
4006.09	W	I	
4013.80	M	I	
4023.70	W	I	

Table 3 (Continued)

Wavelength[a] (Å)	Relative[b] Intensity	Spectrum[c]	Energy levels[d] (cm^{-1})
	Dysprosium (Continued)		
4024.87	VW	I	
4028.42	W	I	
4038.84	VW	I	
4045.99	VS	I	
4048.90	VW	I	
4049.35	VW	I	
4055.01*	VW	I	
4077.98	VW	II	828-25343
4079.27	VW	I	
4085.14	VW	I	
4099.87	VW	I	
4103.88	M	I	
4105.05	VW	II	4756-29109
4105.97*	VW	I	
4126.12	M	I	
4129.13	VW	I	
4130.42	M	I	
4134.14	VW	I	
4134.73	VW	I	
4146.07	M	I	
4167.99	S	I	
4183.73	M	I	
4186.78	VS	I	
4190.90	VW	I	
4191.60	M	I	
4194.85	S	I	
4198.02	W	I	
4201.32	W	I	
4202.25	W	I	
4211.72	VS	I	
4213.18	W	I	
4215.15	M	I	
4218.09	M	I	
4221.10	M	I	
4222.22	VW	I	

Table 3 (Continued)

Wavelength[a] (Å)	Relative[b] Intensity	Spectrum[c]	Energy levels[d] (cm^{-1})
	Dysprosium (Continued)		
4225.14	M	I	
4577.80	W	I	
4589.37	M	I	
4612.28	M	I	
5974.50	M	I	
5988.57	M	I	
6259.09	M	I	
	Holmium		
2518.73	M	II	
2533.80	M	I	
2556.84	M	I	
2586.52	M	I	
2592.99	M	I	
2764.4**	W	I	
2785.7**	W	I	
2940.99	M	I	
3186.37	M	I	
3201.00	M	I	
3206.17	M	I	
3233.34	M	II	
3398.98	W	II	
3414.90	W	II	
3416.46	W	II	
3418.47	W	I	
3424.11	W	I	
3437.04	VW	I	
3449.35	W	I	
3451.23	M	I	
3453.14	VW	II	
3453.85	VW	I	
3456.00	M	I	
3474.26	VW	II	
3484.84	VW	II	

Table 3 (Continued)

Wavelength[a] (Å)	Relative[b] Intensity	Spectrum[c]	Energy levels[d] (cm^{-1})
		Holmium (Continued)	
3507.99	VW	I	
3510.73	M	I	
3515.59	VW	II	
3532.76	VW	I	
3541.41	M	I	
3570.44	M	N	
3579.12	M	I	
3581.83	W	II	
3589.77	VW	N	
3593.07	VW	II	
3599.48	W	I	
3600.95	VW	II	
3605.77	VW	I	
3623.59	VW	I	
3630.91	VW	I	
3641.25	VW	I	
3654.45	VW	II	
3662.29	M	I	
3662.99	M	I	
3666.65	M	I	
3667.97	M	I	
3669.05	VW	II	
3669.52	M	I	
3679.19	W	I	
3679.70	W	I	
3682.65	W	I	
3690.65	VW	I	
3691.95	VW	I	
3694.66	VW	N	
3700.04	VW	I	
3701.27	VW	I	
3709.76	VW	I	
3712.88	VW	I	
3718.62	VW	I	
3720.72	W	N	

Table 3 (Continued)

Wavelength[a] (Å)	Relative[b] Intensity	Spectrum[c]	Energy levels[d] (cm^{-1})
	Holmium (Continued)		
3731.40	W	I	
3732.09	VW	I	
3734.99	VW	N	
3736.35	W	I	
3742.40	VW	I	
3748.17	VW	II	
3769.09	W	I	
3774.1**	W	I	
3774.7**	W	I	
3776.15	VW	I	
3791.55	W	N	
3792.95	W	I	
3796.75	W	I	
3797.26	W	I	
3804.15	W	N	
3810.73	W	I	
3811.86	W	I	
3825.64	W	N	
3829.27	W	I	
3849.88	W	N	
3852.40	VW	II	
3857.72	W	II	
3859.34	VW	N	
3862.62	VW	I	
3890.42	W	I	
3891.02	W	II	
3904.44	W	I	
3909.56	W	I	
3911.80	W	I	
3919.45	W	I	
3938.85	VW	I	
3942.54	VW	I	
3950.56	VW	I	
3955.73	S	I	
3959.68	M	I	

Table 3 (Continued)

Wavelength[a] (Å)	Relative[b] Intensity	Spectrum[c]	Energy levels[d] (cm^{-1})
	Holmium (Continued)		
3975.88	VW	I	
3976.93	VW	I	
3998.29	M	I	
3999.58	VW	I	
4003.39	VW	I	
4027.21	VW	I	
4031.80	M	I	
4037.62	M	I	
4040.81	S	I	
4045.44	VW	II	
4053.93	VS	I	
4068.05	VW	I	
4071.83	VW	N	
4087.35	VW	I	
4087.59	VW	I	
4101.09	S	I	
4103.84	VS	I	
4106.50	VW	I	
4107.36	VW	I	
4108.62	S	I	
4112.00	VW	I	
4120.20	S	I	
4125.65	M	I	
4127.16	S	I	
4134.54	VW	I	
4136.22	W	I	
4163.03	VS	I	
4173.23	S	I	
4194.35	S	I	
4222.29	M	I	
4223.47	M	I	
4227.04	S	I	
4254.43	VS	I	
4264.05	S	I	
4350.73	S	I	

Table 3 (Continued)

Wavelength[a] (Å)	Relative[b] Intensity	Spectrum[c]	Energy levels[d] (cm^{-1})
		Holmium (Continued)	
4934.89	W	I	
4939.01	S	I	
4979.97	S	I	
5860.28	S	I	
5921.76	S	I	
5973.52	M	I	
5982.90	VS	I	
6081.79	S	I	
6305.36	S	I	
		Erbium	
2985.50	M	I	
3331.56*	M	I	
3343.12*	VW	I	
3344.37	W	II	
3366.70	VW	I	
3368.07	VW	II	440-30123
3372.76	W	II	0-29641
3382.06	VW	I	
3383.78*	VW	I	
3399.60*	VW	I	
3422.87	VW	I	
3424.42*	VW	I	
3429.22*	VW	I	
3442.65	W	I	
3446.88	VW	I	
3450.95*	VW	I	
3453.68	VW	I	
3462.58	VW	I	
3464.53	VW	II	
3465.12*	VW	I	
3469.48	W	I	
3476.30*	VW	I	
3480.72*	VW	I	

Table 3 (Continued)

Wavelength[a] (Å)	Relative[b] Intensity	Spectrum[c]	Energy levels[d] (cm^{-1})
		Erbium (Continued)	
3489.36	VW	I	
3499.11	W	II	440-29011
3502.78	VW	I	
3505.70	W	I	
3514.91	VW	II	
3520.03*	W	I	
3522.52	VW	I	
3526.81	VW	I	
3529.57	W	N	
3545.84	W	N	
3556.37	VW	N	
3557.07	VW	N	
3558.02	M	N	
3558.72	W	N	
3563.49	M	N	
3565.15	VW	N	
3569.25	VW	N	
3569.91	VW	N	
3570.74	W	N	
3578.31	VW	N	
3579.44	VW	N	
3580.49	VW	II	440-28361
3585.79*	VW	I	
3586.64	VW	N	
3588.35	VW	N	
3590.73	W	I	
3595.83	VW	I	
3605.69	VW	I	
3607.45	W	I	
3609.44*	VW	I	
3612.40*	VW	I	
3612.56*	VW	I	
3620.18*	W	I	
3627.84*	VW	I	
3628.04	W	I	

Table 3 (Continued)

Wavelength[a] (Å)	Relative[b] Intensity	Spectrum[c]	Energy levels[d] (cm^{-1})
		Erbium (Continued)	
3629.39	VW	I	
3633.26	VW	I	
3634.67	VW	I	
3636.30	VW	I	
3638.69	W	I	
3639.01*	VW	I	
3659.56	VW	I	
3662.86	VW	I	
3664.44	W	I	
3678.95	VW	I	
3684.01	VW	I	
3684.27	VW	II	5133-32267
3692.64	VW	II	440-27514
3694.81*	VW	I	
3697.24	VW	I	
3697.68	VW	I	
3705.77	VW	I	
3706.52	VW	I	
3715.96	VW	I	
3719.31	VW	I	
3747.53	W	I	
3748.99	VW	I	
3756.05	W	I	
3761.94	VW	N	
3768.79	VW	N	
3774.83	VW	I	
3775.28	VW	I	
3778.64	VW	I	
3791.16	VW	N	
3791.53	VW	N	
3792.81	W	I	
3798.24	VW	N	
3798.65	W	I	
3810.33	S	I	
3815.49*	VW	I	

Table 3 (Continued)

Wavelength[a] (Å)	Relative[b] Intensity	Spectrum[c]	Energy levels[d] (cm^{-1})
		Erbium (Continued)	
3826.82*	VW	I	
3830.07*	VW	I	
3849.91	W	N	
3855.93	W	N	
3862.82	VS	I	
3874.73	VW	N	
3892.69	VS	I	
3896.25	VW	II	440-26099
3902.75	W	II	
3903.99	W	I	
3905.44	S	I	
3906.34	W	II	
3937.02	S	I	
3944.41	S	I	
3948.07	VW	II	
3956.43	W	I	
3964.52	W	I	
3973.04	S	I	
3973.60	S	I	
3976.74	VW	I	
3977.03	W	I	
3982.33	W	I	
3987.66	W	I	
4004.07	VW	I	
4007.97	VS	I	
4012.58	VW	I	
4020.52	W	I	
4021.55	VW	I	
4036.12	VW	I	
4037.69	VW	I	
4077.88	VW	I	
4087.65	S	I	
4092.90	VW	I	
4098.11	VW	I	
4123.24*	VW	I	

Table 3 (Continued)

Wavelength[a] (Å)	Relative[b] Intensity	Spectrum[c]	Energy levels[d] (cm^{-1})
		Erbium (Continued)	
4124.80	VW	I	
4131.50	VW	I	
4151.10	VS	I	
4185.45	W	I	
4190.71	M	I	
4218.43	W	I	
4286.56	W	I	
4409.35	M	I	
4426.77	M	I	
4606.62	M	I	
4673.16	W	I	
4722.71	W	I	
4762.66	W	II	
5826.79	W	I	
6221.01	W	N	
6308.79	W	I	
		Thulium[f]	
2973.22++	S	I	0-33624
3046.87++	S	I	0-32811
3081.12++	M	I	0-32446
3172.66++	M	I	0-31510
3180.56++	W	I	0-31432
3233.75++	M	I	0-30915
3241.53++	M	II	0-30841
3291.00	W	II	0-30377
3349.99++	W	I	0-29842
3362.62++	W	II	237-29967
3380.52++	W	I	
3385.09++	W	I	

[f]Lines marked ++ have been reported by Bovey and Garton (3, 4).

Table 3 (Continued)

Wavelength[a] (Å)	Relative[b] Intensity	Spectrum[c]	Energy levels[d] (cm^{-1})
		Thulium (Continued)	
3393.19	VW	I	
3397.50	VW	II	0-29425
3397.87	VW	I	
3410.05^{++}	S	I	0-29317
3412.59^{++}	VW	I	0-29295
3416.59^{++}	S	I	0-29260
3425.08^{++}	W	II	237-29425
3429.33^{++}	VW	I	0-29152
3441.50^{++}	W	II	237-29286
3443.00	VW	I	
3447.35	VW	I	
3453.67^{++}	W	II	237-29183
3462.20^{++}	W	II	0-28875
3467.51	VW	I	
3476.69	W	I	
3480.98	VW	I	
3487.38^{++}	W	I	0-28666
3499.95^{++}	VW	I	0-28564
3514.12^{++}	W	I	0-28449
3517.60^{++}	VW	I	0-28420
3535.52	VW	II	
3537.91	VW	I	
3563.88^{++}	M	I	0-28051
3567.36^{++}	M	I	0-28024
3569.80	VW	I	
3586.07	VW	I	
3598.62	VW	I	
3608.77	VW	II	0-27702
3624.20^{++}	VW	I	0-27584
3638.41^{++}	VW	I	0-27477
3646.70^{++}	M	I	0-27414
3700.26^{++}	VW	II	237-27254
3701.36^{++}	VW	II	0-27009
3717.92^{++}	VS	I	0-26889
3734.12	VW	II	237-27009

Table 3 (Continued)

Wavelength[a] (Å)	Relative[b] Intensity	Spectrum[c]	Energy levels[d] (cm^{-1})
		Thulium (Continued)	
3744.07++	VS	I	0-26701
3751.81++	S	I	0-26646
3761.33++	W	I	0-26579
3761.91++	W	II	0-26575
3781.15++	W	I	0-26440
3795.76++	W	II	237-26575
3798.54	W	I	
3807.72++	W	I	0-26255
3826.38++	M	I	0-26127
3840.87	VW	I	
3848.02++	W	II	0-25980
3883.13++	VS	I	0-25745
3887.35++	VS	I	0-25717
3896.62++	S	I	0-25656
3916.48++	S	I	8771-34297
3949.28++	S	I	8771-34085
4044.47++	W	I	0-24718
4094.19++	VS	I	0-24418
4105.84++	VS	I	0-24349
4138.34++	W	I	0-24157
4158.60	VW	I	8771-32811
4187.62++	VS	I	0-23873
4203.73++	VS	I	0-23782
4359.93++	VS	I	0-22930
4386.43++	S	I	0-22791
4599.02++	M	I	0-21738
4724.26++	M	I	0-21161
4733.34++	S	I	0-21121
5060.90++	S	I	0-19754
5113.99++	M	I	0-19549
5307.12++	S	I	0-18837
5631.40++	S	I	0-17753
5675.85++	S	I	0-17614
5764.30++	S	I	0-17343
5971.28++	S	I	0-16742

Table 3 (Continued)

Wavelength[a] (Å)	Relative[b] Intensity	Spectrum[c]	Energy levels[d] (cm^{-1})
		Ytterbium	
2464.49	VS	I	0-40564
2671.98	S	I	0-37415
2970.56	W	II	0-33654
3289.37	S	II	0-30392
3464.36	VS	I	0-28857
3694.19	M	II	0-27062
3987.98	VS	I	0-25068
		Lutetium[f]	
2989.27++	M	I	0-33443
3081.47++	S	I	1994-34436
3118.43++	M	I	
3171.36++	W	I	0-31523
3278.97++	M	I	0-30489
3281.74++	M	I	1994-32457
3312.11++	M	I	0-30184
3359.56++	M	I	1994-31751
3376.50++	M	I	0-29608
3385.50++	W	I	1994-31523
3396.82++	M	I	
3508.42++	W	I	1994-30489
3567.84++	M	I	0-28020
3636.25++	VW	I	0-27493
3647.77++	VW	I	4136-31542
3841.18++	W	I	1994-28020
3968.46++	VW	I	0-25192
4518.57++	M	I	0-22125
		Scandium	
2974.01	W	I	0-33615
2980.75	W	I	168-33707
3015.36	M	I	0-33154

Table 3 (Continued)

Wavelength[a] (Å)	Relative[b] Intensity	Spectrum[c]	Energy levels[d] (cm^{-1})
		Scandium (Continued)	
3019.34	M	I	168-33279
3255.69	M	I	0-30707
3269.91	S	I	0-30573
3273.63	S	I	168-30707
3907.49	S	I	0-25585
3911.81	S	I	168-25725
3933.38	M	I	168-25585
3996.61	M	I	0-25014
4020.40	S	I	0-24866
4023.69	S	I	168-25014
4054.55	M	I	0-24657
4082.40	M	I	168-24657
		Yttrium	
3552.69	W	I	0-28140
3592.92	M	I	0-27824
3620.94	M	I	530-28140
4039.83	VW	I	0-24747
4047.64	W	I	0-24699
4077.38	W	I	0-24519
4083.71	VW	I	0-24481
4102.38	W	I	530-24900
4128.31	W	I	530-24747
4142.85	W	I	0-24131
4167.52	VW	I	530-24519
4174.14	VW	I	530-24481
		Titanium	
3635.46	M	I	0-27499
3642.68	M	I	170-27615
3653.50	M	I	387-27750
3729.82	M	I	0-26803
3741.06	M	I	170-26893

Table 3 (Continued)

Wavelength[a] (Å)	Relative[b] Intensity	Spectrum[c]	Energy levels[d] (cm^{-1})
		Titanium (Continued)	
3752.86	M	I	387-27026
3948.67	M	I	0-25318
3956.34	M	I	170-25439
3958.21	M	I	387-25644
3981.76	S	I	0-25107
3989.76	S	I	170-25227
3998.64	S	I	387-25388
		Vanadium	
3043.12	W	I	137-32989
3043.56	W	I	0-32847
3044.94	W	I	323-33155
3050.89	W	I	0-32768
3053.65	W	I	0-32738
3056.33	M	I	137-32847
3060.46	M	I	323-32989
3183.41	VS	I	137-31541
3183.98	VS	I	323-31722
3185.40	VS	I	553-31937
3198.01	W	I	137-31398
3202.38	W	I	323-31541
3207.41	W	I	553-31722
3263.24	VW	I	0-30636
3271.64	VW	I	137-30694
3283.31	VW	I	323-30771
3298.14	VW	I	553-30864
3675.70	W	I	2220-29418
3683.13	W	I	2153-29296
3688.07	W	I	2311-29418
3690.28	W	I	2112-29203
3692.22	W	I	2220-29296
3695.86	W	I	2153-29203
3703.58	M	I	2425-29418

Table 3 (Continued)

Wavelength[a] (Å)	Relative[b] Intensity	Spectrum[c]	Energy levels[d] (cm^{-1})
	Vanadium (Continued)		
3704.70	W	I	2311-29296
3705.04	W	I	2220-29203
3778.68	VW	I	2311-28768
3790.32	VW	I	2220-28596
3794.96	W	I	2425-28768
3799.91	W	I	2193-28462
3808.52	W	I	0-26249
3813.49	W	I	137-26353
3818.24	W	I	0-26183
3828.56	W	I	137-26249
3840.75	M	I	323-26353
3844.44	W	I	0-26004
3847.33	W	I	137-26122
3855.37	M	I	0-25931
3855.84	W	I	553-26480
3864.86	W	I	137-26004
3867.60	W	I	323-26172
3875.08	W	I	323-26122
3875.90	W	I	137-25931
3876.09	W	I	553-26345
3890.18	W	I	323-26022
3892.86	W	I	323-26004
3902.25	M	I	553-26172
3909.89	W	I	553-26122
4092.69	W	I	2311-26738
4099.80	W	I	2220-26605
4105.17	W	I	2153.26506
4109.79	W	I	2112-26438
4111.78	M	I	2425-26738
4115.18	W	I	2311-26605
4116.47	W	I	2220-26506
4123.57	W	I	2153-26397
4128.07	W	I	2220-26438
4132.02	W	I	2311-26506
4134.49	W	I	2425-26605

Table 3 (Continued)

Wavelength[a] (Å)	Relative[b] Intensity	Spectrum[c]	Energy levels[d] (cm^{-1})
		Niobium	
3580.27	VW	I	1050-28973
4058.94	W	I	1050-25680
4079.73	W	I	695-25200
4100.92	W	I	392-24770
4123.81	VW	I	154-24397
4137.10	VW	I	0-24165
4139.71	VW	I	1050-25200
4152.58	VW	I	695.24770
4163.66	VW	I	154-24165
4164.66	VW	I	392-24397
4168.13	VW	I	0-23985

III. IMPLICATIONS OF RESULTS

A. The Role of the Free Atom

As dramatically attested by Figures 6 and 7, the fuel-rich oxygen-acetylene flame clearly provides an environment more favorable for the existence of free-atoms of those elements that have a strong predilection to form stable monoxide molecules in stoichiometric flames. Furthermore, the favorability of the environment as a function of oxygen/fuel ratio decidedly parallels the enhancements in atomic emission spectra (44). Both atomic emission and absorption show maximal signal in the cooler fuel-rich flame. This evidence leaves little doubt that these phenomena are the manifestation of a chemical mechanism, i.e., a purely thermal mechanism cannot be invoked to explain the character of the fuel-rich oxygen-acetylene flame spectra. Doubtless, the enhancements in lanthanide emission spectra in fuel-rich oxygen-acetylene flames can be attributed to the observed increase in free-atom populations. This inference provides the framework upon which a requisite theory can be constructed.

Inspection of the excitation potential data available for the rare earth lines excited in the oxygen-acetylene

B. A Possible Flame Mechanism

It probably is unrealistic to expect that one simple mechanism could account for the complicated sequence of events that take place when a solution is aspirated into a flame. The evaporation of the solvent is most likely the first step, followed by the melting, vaporization, and dissociation of the metal salt. Thermal dissociation of the metal salt should result in a mixture of products which includes free metal atoms, monoxide molecules, and other molecular species. It is extremely difficult to estimate the relative yield of free-atoms and monoxide molecules. The degree of efficiency of free-atom production may be revealed by information on the fraction-of-atoms-available near the burner tip (45). Indeed, a systematic study of the fraction-of-atoms-available along the entire length of the flame would be valuable. The dissociation products may react in the various zones of the flame with the combustion gases and their products or may also react with the other chemical species, including atoms, molecules, free-radicals, or ions present. Finally the excitation of the various particles takes place. These events occur in less than one to ten

milliseconds.

It is well known that fuel-rich hydrocarbon flames contain appreciable concentrations of atomic carbon, solid carbon, CH-radicals, C_2, C_3, and other carbon containing species (46). It also is known that the reaction of atomic oxygen with these species is highly exothermic. Therefore, it is not surprising that the atomic oxygen concentration in these flames is considerably less than in stoichiometric flames (47). The consequences of a reduction in atomic oxygen concentration can be two-fold. If free-atoms are formed as the major product of the thermal dissociation of the metal salt, one would expect some degree of free-atom accumulation due to the reduced probability of their collision with atomic oxygen. Or if the oxide does happen to be the degradation product of the original solid residue, the much lower atomic oxygen concentration in the flame allows the oxide thermal dissociation equilibrium to be favorably shifted to a higher concentration of free-atoms of the metal.

Another mechanism appears to be worthy of consideration. A number of chemical reactions have been suggested to account for flame chemiluminescence phenomena, several of which have a direct bearing on the production of free metal atoms in

flames (48-50). The most attractive of the proposed mechanisms will be briefly sketched in the paragraphs to follow.

Broida and Shuler (51) suggested that an excited intermediate conveys the energy released in the combustion process into a chemiluminescence reaction. Since it is unnecessary to invoke chemiluminescence to account for the lanthanide flame spectra, the energy carried by the intermediate can be used for oxide dissociation. As suggested by Gilbert (52), the most likely species to carry the energy released in the combustion process is the hydronium ion, now known to account for seventy to ninety percent of the positive ions in the reaction zone of a premixed oxygen-acetylene flame (53-56). (The negative ions are practically all electrons.) Hydronium ions reportedly are produced homogeneously in the reaction zone and persist farther downstream into the burned gases than any other flame ion (57). Although similar information is not available on the oxygen-acetylene diffusion flame, it is reasonable to expect its ill-defined reaction region also to be abundant with hydronium ions.

Two important facts emerge from recent quantitative mass spectrometric investigations of Bascombe, Green, and Sugden

(57). First, the hydronium ion is definitely a genuine flame ion; whereas, the formation of mono and dihydrates of the hydronium ion appear to be secondary phenomenon associated with the sampling technique. Second, the controlled addition of up to one percent of acetylene to oxygen-hydrogen flames affords a striking increase in hydronium ion concentration.

Berendsen, Taelemans, and Van Tiggelen (58) also report that the addition of small amounts of hydrocarbon to oxygen-hydrogen flames produces a remarkable increase in positive ion concentration. Knewstubb and Sugden (59, 60) have reported the presence of hydronium ions in oxygen-hydrogen flames with no acetylene additive. These observations were later (57) attributed to the presence of hydrocarbon impurities in the fuel although the literature is not clear on this point. It is notable that mass spectrometric studies on clean nitrous oxide supported flames reveal a conspicuous absence of the hydronium ion (61, p. 285).

The question may arise as to whether the ions detected by mass spectrometric probing truly reflect the ionic composition of the flame under investigation. For an appraisal of these techniques, the reader is referred to a paper by

Knewstubb and Sugden (60) who discuss in detail the reliability of mass spectrometric flame measurements.

According to the arguments of Feuno et al. (62), the presence of the acetylene molecule is prerequisite to the formation of abundant hydronium ions in hydrocarbon flames. Calcote (63), using the Langmiur probe method, claims that for the same composition of combustible mixture the positive ion concentration is greater in the acetylene flame than in any other hydrocarbon flame. It appears at this point that, at least to some degree, a unique property of acetylene is its ability to enter into combustion processes wherein the hydronium ion is a favored product.

Calcote and King (63, 64) report that the peak hydronium ion concentration is much higher in hydrocarbon flames operated under slightly fuel-rich conditions. Unfortunately, the observations by Calcote were made on very low pressure, premixed air acetylene flames. It may be presumptuous to expect parallel behavior for the hydronium ions in an oxygen-acetylene flame burning at atmospheric pressure. Information on the hydronium ion concentration as a function of oxygen/fuel ratio in the latter mentioned flame would be very valuable.

A likely reaction between the plentiful oxide molecules and the most abundant ion (H_3O^+) now can be written to account for the increase in metal atoms in the flame.

$$H_3O^+ + MO + e = H_2O + OH + M^o$$

The exact amount of energy liberated by this reaction is uncertain. For the above reaction, ΔH^o should range from - [10.3 to 13.1] + D(MO) ev. depending on the value selected for the heat of formation of the hydronium ion (65, 66). For ytterbium and europium this mechanism is even more attractive. Gilbert (67) has speculated that these elements form hydroxide molecules in the flame instead of forming monoxide molecules; the reaction in this case would be:

$$H_3O^+ + MOH + e = 2\ H_2O + M^o$$

As mentioned previously, only rare earth lines originating in low lying electronic terms are observed in emission from the fuel-rich oxygen-acetylene flame. This observation suggests that little chemical energy is available for electronic excitation. There is no reason to suppose that all of the excess energy must go into atomic electronic excitation. The molecular products in these reactions help to balance the energy budget by leaving the reaction scene in

vibrationally excited states. Nevertheless, it is difficult to see why some fraction of the excess energy is not left over for electronic excitation. This presents one of the major objections to this mechanism. A study of the energy distribution in OH and H_2O might be informative in this respect.

In the absence of more detailed experimental information regarding the production of free metal atoms in the fuel-rich oxygen-acetylene flame, it does not seem possible at the present time to begin to resolve the relative contributions of the several mechanisms proposed.

C. Suggestions for Further Investigation

The foremost question regarding the production of free-atoms in the fuel-rich environment concerns the relative yield of free metal atoms and oxide molecules in the thermal degradation of residual salt particles. If the great majority of the free metal atoms are produced directly from the residue, it will not be necessary to invoke a chemical reduction mechanism. A quantitative study of atomic and molecular absorption (salts and oxides) along the flame axis close to the burner tip may be informative.

One of the noticeable features of Table 3 is the remarkable number of ion lines, many of which are quite strong. This surprising result indicates that there must be a significant accumulation of metal ions in the flame. The behavior of the ion lines with changes in flame conditions parallels the behavior of the neutral atom lines. Whether the ions form directly from a molecular species or result from thermal ionization of neutral atoms is an open question. In view of the numerous reports of chemi-ionization in the hydrocarbon flames (68-70), the former possibility should not be precluded as a possible scheme. Conceivably, the relatively low ionization potentials for the lanthanide elements could account for these observations. A quantitative study of the relative populations of ions and neutral atoms may shed some light on this matter. Feasibly, the hydronium ion could be involved in the ionization process by the following reaction:

$$H_3O^+ + MO = H_2O + OH + M^+ \rightleftharpoons e + M^o$$

In the above scheme, the short lived incipient ions feed the neutral atom population by electron capture. There are no

Table 4. Dissociation energies of rare earth monoxides, and ionization potentials of neutral rare earth atoms

Element	D_o (ev.)	I.P. (ev.) (42)
Lanthanum	8.4 (71)[a]	5.58
Cerium	8.3 (72)[a]	5.55
Praseodymium	7.7 (72)[a]	5.55
Neodymium	7.4 (71, 72)[a]	5.42
Samarium	6.1 (73)	5.55
Europium	--	5.64
Gadolinium	5.9 (74)	6.14
Terbium	--	--
Dysprosium	--	6.16
Holmium	--	--
Erbium	--	6.17
Thulium	--	6.16
Ytterbium	--	6.16
Lutetium	5.3 (74)	6.12
Scandium	7 (74)	6.53
Yttrium	7.0 (73)	6.50

[a]White, D., Columbus, Ohio. Revised values. Private communication. 1961.

markedly reduce the hydronium ion concentration (60, 75). This could be due to the destruction of hydronium ions by dissociative recombination with the increased number of electrons or by chemi-ionization of the alkali metal reacting with hydronium ions. Since the supply of hydronium ions is known to be decreased by the presence of alkali metals, the addition of small amounts of cesium, for example, should cause a marked reduction in lanthanide free atoms (if hydronium ions are involved in their formation). On the other hand, the lanthanide neutral atom population should increase at the expense of the ionic population when the electron density in the flame is increased by addition of small quantities of alkali metal. A study of these effects should be very interesting and informative.

IV. ANALYTICAL APPLICATIONS

A. Preliminary Observations

Inasmuch as a number of the lanthanide elements exhibit very large cross sections for the capture of thermal neutrons, the detection and determination of elements in this group are of vital importance in nuclear fuel technology. In general, the quantities of impurities are so small and the chemical behavior so similar that the use of chemical analysis is often out of the question. Emission spectrographic methods, heretofore, have provided most of the analytical information on the analysis of rare earth mixtures. In these methods the use of highly energetic sources excite upward to 100,000 lines in complex mixtures of the rare earth elements; thus, spectral interferences are not uncommon. The problem of isolating a single line of spectral purity having the requisite characteristics for quantitative analysis is compounded by the rather uniform distribution of intensity prevailing over the maze of spectral lines. This difficulty largely has been overcome by the successful application of flame photometry to rare earth analysis. There are, however, a number of special problems associated with flame photometry.

Since the energy for spectral excitation derives from the energy released in the flame combustion process, emission flame photometry, in general, is limited to those elements whose lines have relatively low excitation potentials. Fortunately, fuel-rich oxygen-acetylene flames are sufficiently energetic to excite an ample number of rare earth lines. The limitation imposed by flame energetics, however, can be of importance in the analysis of rare earth samples for common impurities. In atomic absorption the sensitivity is essentially independent of excitation potential; hence, elements of high excitation potential can be determined as readily as elements that are easy to excite (76, 77).

Emission flame photometry also can be subject to excitation interferences caused by changes in the effective electronic temperature of the radiating vapor. Excitation interferences are usually due to the presence of other atoms having lower excitation potentials. So far as anomalous excitation effects observed in emission are caused by variations in the distribution of atoms over the various excited states, interferences stemming from such variations would have no counterpart in absorption. There are no examples in spectrochemical analysis in which such excitation inter-

Knewstubb and Sugden (60) who discuss in detail the reliability of mass spectrometric flame measurements.

According to the arguments of Feuno et al. (62), the presence of the acetylene molecule is prerequisite to the formation of abundant hydronium ions in hydrocarbon flames. Calcote (63), using the Langmiur probe method, claims that for the same composition of combustible mixture the positive ion concentration is greater in the acetylene flame than in any other hydrocarbon flame. It appears at this point that, at least to some degree, a unique property of acetylene is its ability to enter into combustion processes wherein the hydronium ion is a favored product.

Calcote and King (63, 64) report that the peak hydronium ion concentration is much higher in hydrocarbon flames operated under slightly fuel-rich conditions. Unfortunately, the observations by Calcote were made on very low pressure, premixed air acetylene flames. It may be presumptuous to expect parallel behavior for the hydronium ions in an oxygen-acetylene flame burning at atmospheric pressure. Information on the hydronium ion concentration as a function of oxygen/fuel ratio in the latter mentioned flame would be very valuable.

A likely reaction between the plentiful oxide molecules and the most abundant ion (H_3O^+) now can be written to account for the increase in metal atoms in the flame.

$$H_3O^+ + MO + e = H_2O + OH + M^o$$

The exact amount of energy liberated by this reaction is uncertain. For the above reaction, ΔH^o should range from - [10.3 to 13.1] + D(MO) ev. depending on the value selected for the heat of formation of the hydronium ion (65, 66). For ytterbium and europium this mechanism is even more attractive. Gilbert (67) has speculated that these elements form hydroxide molecules in the flame instead of forming monoxide molecules; the reaction in this case would be:

$$H_3O^+ + MOH + e = 2\ H_2O + M^o$$

As mentioned previously, only rare earth lines originating in low lying electronic terms are observed in emission from the fuel-rich oxygen-acetylene flame. This observation suggests that little chemical energy is available for electronic excitation. There is no reason to suppose that all of the excess energy must go into atomic electronic excitation. The molecular products in these reactions help to balance the energy budget by leaving the reaction scene in

vibrationally excited states. Nevertheless, it is difficult to see why some fraction of the excess energy is not left over for electronic excitation. This presents one of the major objections to this mechanism. A study of the energy distribution in OH and H_2O might be informative in this respect.

In the absence of more detailed experimental information regarding the production of free metal atoms in the fuel-rich oxygen-acetylene flame, it does not seem possible at the present time to begin to resolve the relative contributions of the several mechanisms proposed.

C. Suggestions for Further Investigation

The foremost question regarding the production of free-atoms in the fuel-rich environment concerns the relative yield of free metal atoms and oxide molecules in the thermal degradation of residual salt particles. If the great majority of the free metal atoms are produced directly from the residue, it will not be necessary to invoke a chemical reduction mechanism. A quantitative study of atomic and molecular absorption (salts and oxides) along the flame axis close to the burner tip may be informative.

One of the noticeable features of Table 3 is the remarkable number of ion lines, many of which are quite strong. This surprising result indicates that there must be a significant accumulation of metal ions in the flame. The behavior of the ion lines with changes in flame conditions parallels the behavior of the neutral atom lines. Whether the ions form directly from a molecular species or result from thermal ionization of neutral atoms is an open question. In view of the numerous reports of chemi-ionization in the hydrocarbon flames (68-70), the former possibility should not be precluded as a possible scheme. Conceivably, the relatively low ionization potentials for the lanthanide elements could account for these observations. A quantitative study of the relative populations of ions and neutral atoms may shed some light on this matter. Feasibly, the hydronium ion could be involved in the ionization process by the following reaction:

$$H_3O^+ + MO = H_2O + OH + M^+ \rightleftharpoons e + M^O$$

In the above scheme, the short lived incipient ions feed the neutral atom population by electron capture. There are no

serious energetic restrictions on this reaction, a deduction consistent with the values for the rare earth monoxide dissociation energies and for the neutral atom ionization potentials as given in Table 4. Since the flame processes governing the character of the lanthanide emission spectra do not require non-equilibrium conditions for their fulfillment, the slight exothermic nature of the above reaction neatly fits the observations. It is noteworthy that the above reaction does not go via a three-body collision. In view of these arguments, this mechanism merits further exploration.

If the hydronium ion mechanism is to play an important role in the production of free atoms in the fuel-rich environment, the rate at which metal atoms are liberated from their monoxide molecules must exceed the rate of oxide reformation. It is doubtful that more than a small fraction of metal atoms present in the flame find their way into the free atomic state. Possibly, the rate determining step in the sequence of events leading to the production of free atoms and(or) ions is the rate of formation of hydronium ions in the flame and not the rate of reduction of monoxide molecules. Reportedly, small additions of alkali metals into flames

Table 4. Dissociation energies of rare earth monoxides, and ionization potentials of neutral rare earth atoms

Element	D_o (ev.)	I.P. (ev.) (42)
Lanthanum	8.4 (71)[a]	5.58
Cerium	8.3 (72)[a]	5.55
Praseodymium	7.7 (72)[a]	5.55
Neodymium	7.4 (71, 72)[a]	5.42
Samarium	6.1 (73)	5.55
Europium	--	5.64
Gadolinium	5.9 (74)	6.14
Terbium	--	--
Dysprosium	--	6.16
Holmium	--	--
Erbium	--	6.17
Thulium	--	6.16
Ytterbium	--	6.16
Lutetium	5.3 (74)	6.12
Scandium	7 (74)	6.53
Yttrium	7.0 (73)	6.50

[a]White, D., Columbus, Ohio. Revised values. Private communication. 1961.

markedly reduce the hydronium ion concentration (60, 75). This could be due to the destruction of hydronium ions by dissociative recombination with the increased number of electrons or by chemi-ionization of the alkali metal reacting with hydronium ions. Since the supply of hydronium ions is known to be decreased by the presence of alkali metals; the addition of small amounts of cesium, for example, should cause a marked reduction in lanthanide free atoms (if hydronium ions are involved in their formation). On the other hand, the lanthanide neutral atom population should increase at the expense of the ionic population when the electron density in the flame is increased by addition of small quantities of alkali metal. A study of these effects should be very interesting and informative.

IV. ANALYTICAL APPLICATIONS

A. Preliminary Observations

Inasmuch as a number of the lanthanide elements exhibit very large cross sections for the capture of thermal neutrons, the detection and determination of elements in this group are of vital importance in nuclear fuel technology. In general, the quantities of impurities are so small and the chemical behavior so similar that the use of chemical analysis is often out of the question. Emission spectrographic methods, heretofore, have provided most of the analytical information on the analysis of rare earth mixtures. In these methods the use of highly energetic sources excite upward to 100,000 lines in complex mixtures of the rare earth elements; thus, spectral interferences are not uncommon. The problem of isolating a single line of spectral purity having the requisite characteristics for quantitative analysis is compounded by the rather uniform distribution of intensity prevailing over the maze of spectral lines. This difficulty largely has been overcome by the successful application of flame photometry to rare earth analysis. There are, however, a number of special problems associated with flame photometry.

Since the energy for spectral excitation derives from the energy released in the flame combustion process, emission flame photometry, in general, is limited to those elements whose lines have relatively low excitation potentials. Fortunately, fuel-rich oxygen-acetylene flames are sufficiently energetic to excite an ample number of rare earth lines. The limitation imposed by flame energetics, however, can be of importance in the analysis of rare earth samples for common impurities. In atomic absorption the sensitivity is essentially independent of excitation potential; hence, elements of high excitation potential can be determined as readily as elements that are easy to excite (76, 77).

Emission flame photometry also can be subject to excitation interferences caused by changes in the effective electronic temperature of the radiating vapor. Excitation interferences are usually due to the presence of other atoms having lower excitation potentials. So far as anomalous excitation effects observed in emission are caused by variations in the distribution of atoms over the various excited states, interferences stemming from such variations would have no counterpart in absorption. There are no examples in spectrochemical analysis in which such excitation inter-

ferences can be isolated from interferences that arise from interelement effects chiefly chemical in nature. The latter probably represent the greatest obstacle to further progress toward the perfection of methods employing a flame. Chemical interferences become manifest through the reduction of the number of atoms available for excitation (or absorption). The lanthanide elements, notorious for forming stable monoxide molecules in conventional flames, provide an example of one kind of chemical interference. Numerous chemical interferences not involving oxide formation, however, can be found in the literature (78-82). Some progress toward a partial solution has been realized when reagents have been added to the sample to produce compensating reactions in the flame. Here absorption methods may be preferable to emission methods since additional reagents may introduce interferences that may be more pronounced in emission than in absorption (83-87). Finally, the sensitivity of emission flame photometry can be reduced by self-absorption in the flame; whereas, in atomic absorption the effect of self-absorption contributes to the spectrum and in no sense reduces the sensitivity. Although it is not expected that atomic absorption spectroscopy will replace the conventional flame

emission methods, there is promise that some of the limitations on the emission methods may be overcome through the use of this relatively new technique of analysis.

As a means of estimating the analytical potentialities of the atomic absorption spectra reported earlier, exploratory experiments were conducted in which the atomic absorption spectra of vanadium, titanium, niobium, scandium, yttrium, and rhenium were photographed at various concentrations of metal in the flames. The wavelengths of the strongest lines of these elements and their sensitivities of detection are summarized in Table 5. The latter are expressed as the concentrations required to produce a visually detected absorption line. It is evident from the results that these lines exhibit adequate sensitivity to satisfy many analytical requirements.

Although the photographic technique described earlier is a good scheme to use for survey studies, it is not a particularly sensitive method for analytical investigations. Probably the most important reason for this lack of sensitivity is that flame emission lines are superposed directly on the atomic absorption lines. Commercial atomic absorption spectrophotometers, with photoelectric detection, circumvent

Table 5. Wavelengths and photographic detection sensitivities of the strongest absorption lines of several elements of interest

Element	Wavelength (Å)	Sensitivity (ppm by weight in solution)
Vanadium	3183.41	25
	3183.98	10
	3185.40	25
	3828.56	100
	3840.75	100
	3855.84	50
	3902.25	100
	4111.78	100
	4379.24	50
	4384.72	100
	4389.97	100
Titanium	3635.46	100
	3642.68	50
	3653.50	50
	3729.82	100
	3741.06	50
	3948.67	100
	3752.86	50
	3956.34	100
	3958.21	100
	3981.76	100
	3989.76	100
	3998.64	50
Niobium	4058.94	250
	4079.73	250
	4100.92	250
Scandium	3255.69	50
	3269.91	10
	3273.63	10
	3907.49	5
	3911.81	5
	3933.38	100

Table 5 (Continued)

Element	Wavelength (Å)	Sensitivity (ppm by weight in solution)
	4020.40	5
	4023.69	5
	4054.55	50
	4082.40	50
Yttrium	4077.38	50
	4102.38	100
	4128.31	100
	4142.85	100
Rhenium	3451.88	50
	3460.46	25
	3464.73	25

this problem by modulating the incident radiation before it reaches the atomic vapor and by amplifying the output of the detector by an amplifier tuned to this modulation frequency. Thus, the radiation emitted by the atomic vapor produces no signal at the output of the amplifier. A further effect tending to reduce the sensitivity of the photographic method is the photographic halation arising from the continuum border on each side of the absorption line. Besides the loss in analytical sensitivity, any advantage that atomic absorption may have over methods requiring high dispersion

equipment is defeated if the photographic technique is employed. From the foregoing, it is natural to look first to commercial instrumentation to further explore the usefulness of the observed atomic absorption spectra.

The Perkin-Elmer Model-214 represents a typical commercial atomic absorption spectrophotometer. The design of the Model-214 incorporates the use of an electrically modulated hollow-cathode lamp as the line source, double-beam optics, a.c. amplification to discriminate against flame emission, and a grating monochromator. The optical arrangement permits the source light to make a single pass through the flame of a ten centimeter air-acetylene burner similar to that described by Clinton (88). Since a complete description of the Model-214 can be obtained from the manufacturer, no further description will be given here. The results of extensive experimentation with the Perkin-Elmer Model-214 are summarized briefly below.

Since hollow-cathode lamps were available only for lanthanum, gadolinium, samarium, yttrium, vanadium, and titanium, these were the only elements studied. Although the latter four elements could be detected below the 50 ppm level, it soon became apparent that the Model-214 suffered

from a lack of versatility. The most troublesome feature of the Model-214, and indeed with all commercial atomic absorption spectrophotometers, centers around the hollow-cathode lamp. Of the six lamps studied, the yttrium lamp gave the most intense emission lines. The experimental facility described by Fassel et al. (24) was used to compare quantitatively the intensity of the yttrium spectrum emitted from a hollow-cathode lamp, a fuel-rich oxygen-acetylene flame fed with 1000 ppm ethanolic yttrium perchlorate solution, and an yttrium iodide microwave driven electrodeless discharge lamp similar to the type described by Corliss et al. (89). The relative intensities of the sources in the order mentioned above were in the proportion $1:1.5:10^3$. Each of the hollow-cathode discharge lamps studied, besides emitting such a weak spectrum, had an average useful life of less than fifteen hours. The poor quality and high cost of the rare earth hollow-cathode lamps coupled with the fact that a different lamp is needed for each element of interest makes their use impractical for studying the atomic absorption spectra of the lanthanides. An atomic absorption instrument suitable for exploratory research should be of such flexibility that the instrument can be used in conjunction with nearly any variety

of light source. Unfortunately, the Perkin-Elmer Model-214 fails to meet this requirement.

The photographic technique described earlier was used to demonstrate that an atomic vapor of the aforementioned elements was produced more effectively with a fuel-rich oxygen-acetylene diffusion flame than with the Clinton type air-acetylene flame (88). Hence the Model-214 was re-equipped with the triple burner system described earlier. Unfortunately, the turbulent incandescent flame of the Beckman burner gave rise to a very high noise level when used with the Model-214. With three flames the recorded noise was approximately ten percent (absorption units). This high noise level prompted the author to attempt using a pre-mixed oxygen-acetylene flame produced by a burner described by Kniseley et al. (90). Actually, the burner design was modified to be more suitable for atomic absorption. An increase in the width of the premixing channel furnished a flame of broader dimension. Also, through the expedient of a snap-on premixing attachment, the procedure for aligning the burner was circumvented. The design of the burner used in the experiments with the Model-214 is given in Figure 8. Examination of the flame produced by a Beckman burner

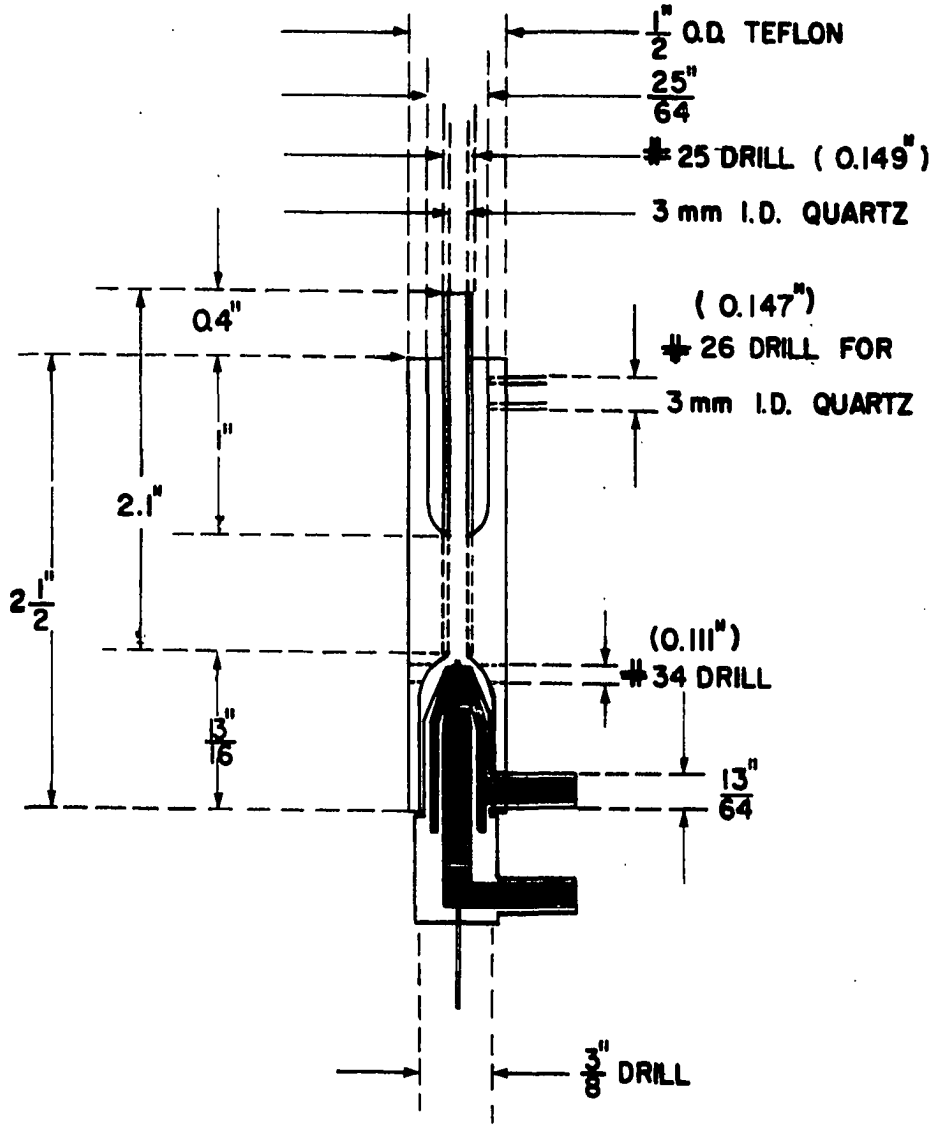

Figure 8. Premix burner attachment

equipped with a snap-on premixing attachment will reveal three definite zones. The primary reaction zone, being somewhat incandescent, gave a high noise level and low absorption. The interconal zone always gave the maximal signal/noise ratio. This zone corresponded to approximately 37 mm above the burner tip. Absorption was undetected in the panache of the flame. In general, absorption was slightly lower in the premixed flames than in the diffusion flames; the signal/noise ratio, however, was increased by nearly an order of magnitude.

The light beam traversing the flames of three burners in tandem represents the maximal path length attainable with the Model-214. The optical arrangement of the Model-214 precludes any possibility of adapting the instrument to multipass operation, another limitation of this design.

With the above desirable features in mind, an atomic absorption spectrophotometer was fashioned from available components of a Perkin-Elmer Model-13 infrared spectrophotometer. The scheme to be described in the following paragraphs combines dual-beam, multipass optics with a.c. amplification and scale expansion into an instrument of such flexibility that it can be used in conjunction with an a.c.

or d.c. source as an atomic absorption spectrophotometer or as an emission spectrometer.

B. Instrumentation

Conversion of the Perkin-Elmer Model-13 infrared spectrophotometer into an atomic absorption instrument for operation in the ultraviolet and visible regions involved drastic modifications in the source, optics, and detector with concomitant minor alterations in the electronics. A block diagram of the modified instrument is given in Figure 9.

1. Source

In his early papers, Walsh (7, 8) maintained that it is scarcely feasible to use a continuous source for atomic absorption measurements for the following reasons: (a) The isolation of an atomic absorption line from a continuous background requires a monochromator of much higher resolving power than is otherwise necessary. (b) The energy emitted over such a small spectral slit-width would be much too low to give a high enough signal/noise ratio. Walsh further suggested that the absorption coefficient at the center of the line could be measured with a source which emits lines having a much smaller half-width than the absorption line. Before

Figure 9. Block diagram, complete instrument

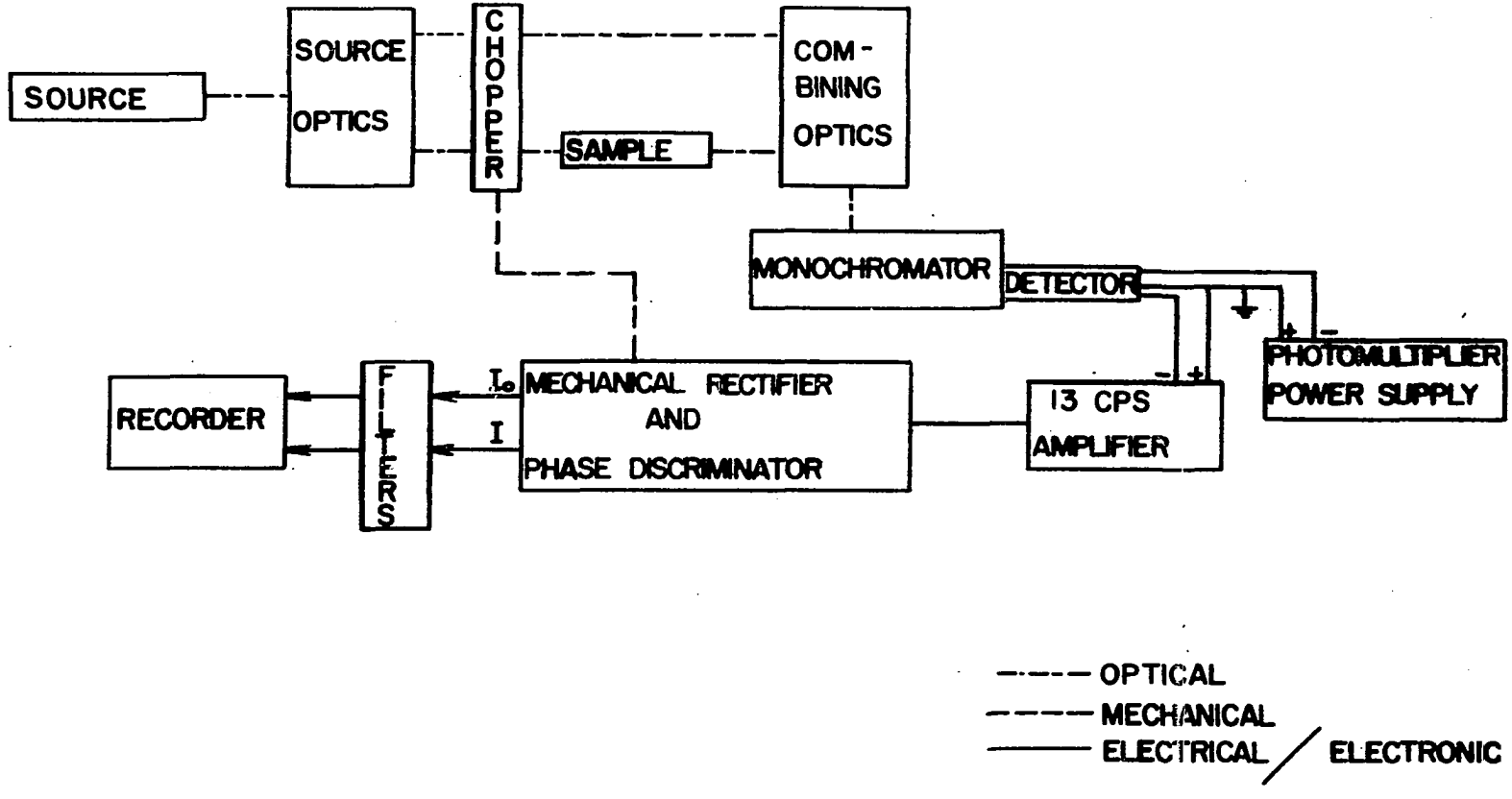
SOURCE
SOURCE OPTICS
CHOPPER
SAMPLE
COM-BINING OPTICS
MONOCHROMATOR
DETECTOR
PHOTOMULTIPLIER POWER SUPPLY
13 CPS AMPLIFIER
MECHANICAL RECTIFIER AND PHASE DISCRIMINATOR
I_o
I
FILTERS
RECORDER
OPTICAL
MECHANICAL
ELECTRICAL / ELECTRONIC

considering specific sources in detail, it is instructive to examine the conditions that must be fulfilled by a lamp which is to be used for atomic absorption measurements.

In an ordinary spectroscopic light source, such as a flame or an arc, there is a hot center region where most of the electrical or thermal excitation takes place. A cooler, less excited blanket encompasses the hot center region and is capable of absorbing some of the light emitted. Radiation emitted by the center is subjected to a greater degree of Doppler broadening than the outer part. Consequently, the absorption line originating in the outer region is narrower than the emission line from the center of the discharge. A line emitted from a source under these conditions consists of a distribution of intensity which has a minimum at the center flanked by a maximum on either side. Such a line is said to be "self-reversed". It is essential that a sharp line-source used for atomic absorption exhibit little or no self-reversal since precisely that missing portion of a self-reversed line is the radiation sensitive to the atomic concentration in the absorbing vapor. This is the most important requirement for an effective atomic absorption source. Several practical features of a good source include high

intensity, stable radiant output, and long life.

It has been shown that sealed off hollow-cathode lamps of the type used in analytical atomic absorption exhibit appreciable self-reversal--even for those of high melting point metals such as copper and chromium (91). For low melting point cathodes, such as cadmium or zinc, the degree of self-reversal can be severe. In such cases the flame absorption is critically dependent on the current through the hollow-cathode lamp. Often experimental conditions are difficult to reproduce because lamp characteristics change with use (92-94). Because cathode lamps seem to be fraught with difficulties, the possibility of utilizing a microwave driven discharge as a source in atomic absorption was explored.

Low pressure (0.01 to 20 torr) electrodeless discharge lamps were prepared for all of the rare earth iodides according to the method of Corliss et al. (89). The line spectra emitted from these lamps were very sharp, extremely intense (at least 1000 times as intense as a hollow-cathode lamp rated for fifteen milliampere), and free from background and self-reversal. Unfortunately, the radiant output of these lamps was most unstable, and the life of each of the lamps

was very short (from less than one hour up to several hours).

A technique was developed that did not require a volatile salt; also, the need to seal off the tube at a fixed pressure was unnecessary. Here, the elemental metal was used in a tube open to a gas system in which the pressure could be varied from 0.1 torr to atmospheric pressure. Argon was used as the supporting gas. Preparation of the lamps was very simple, requiring only a few minutes. For operation, the lamps were immersed in the field of a resonant cavity (Ophthos Instrument Company). A 100-watt Microtherm unit (Raytheon Mfg. Co.), designed to operate at 2450 Mc, powered the cavity. The discharge was initiated at a pressure of approximately 10 torr. When carrier gas was passed into the lamp slowly, the argon spectrum emitted by the discharge gave way to a fully developed metal spectrum. The discharge was stable enough for absorption measurements to be made with dual-beam optics. Furthermore, the useful life of each of the discharge lamps was found to be greater than thirty-five hours of nearly continuous operation. Unfortunately, the extremely intense spectra emitted by these lamps were found to be highly self-reversed. After extensive investigation, this system was abandoned.

Probably because of Walsh's arguments presented in the early papers on atomic absorption, very little work on the use of a spectral continuum as a source has appeared in the literature. Allan (95), who worked with photographic detection and relatively high dispersion equipment, used tungsten and hydrogen continua to determine the detection limits for several common elements in the air-acetylene flame. Gibson et al. (96, p. 288) claim some measure of success with a tungsten lamp used in conjunction with photoelectric detection, but the technique has not been applied to practical analysis. Seemingly, the use of a spectral continuum as a source is worthy of investigation.

The source selected for the remainder of this work was a 150-watt, d.c. xenon compact arc lamp (Hanovia Chemical and Mfg. Co., #901C1). The average life of the lamp is quoted by the manufacturer to be approximately 1000 hours. The lamp was of such intensity that more than sufficient energy was available when a spectral band pass as small as 0.05 Å in the visible region was monitored. The high frequency noise emanating from the xenon arc amounted to less than one percent of the total radiant output. The dual-beam optics easily compensated for the low frequency fluctuations, which were

less than two percent.

2. Chopper

A large single-bladed semicircular chopper driven by a synchronous motor interrupted both sample and reference beams alternately at 13 cps. The original Perkin-Elmer chopper assembly and mechanical rectifier (breaker) assembly were retained. The angles at which the light traversed the flames were minimized when the radius of the chopper blade was decreased to nine centimeters.

3. Optics

The Perkin-Elmer Model-13 may be operated as a double-beam instrument to record transmittance ratio or as a single beam emission spectrometer in which the available radiant energy is more efficiently utilized. The functioning of the optical system will vary in accordance with the mode of operation selected. A schematic diagram of the optical arrangement is shown in Figure 10. The specifications on all of the optical elements are given in Table 6.

When the normal ratio-recording mode was used, the stationary beam-splitting mirror B directed half of the available energy through the plane of the chopper into the multipass area where an image of the source was formed on the

Figure 10. Optics

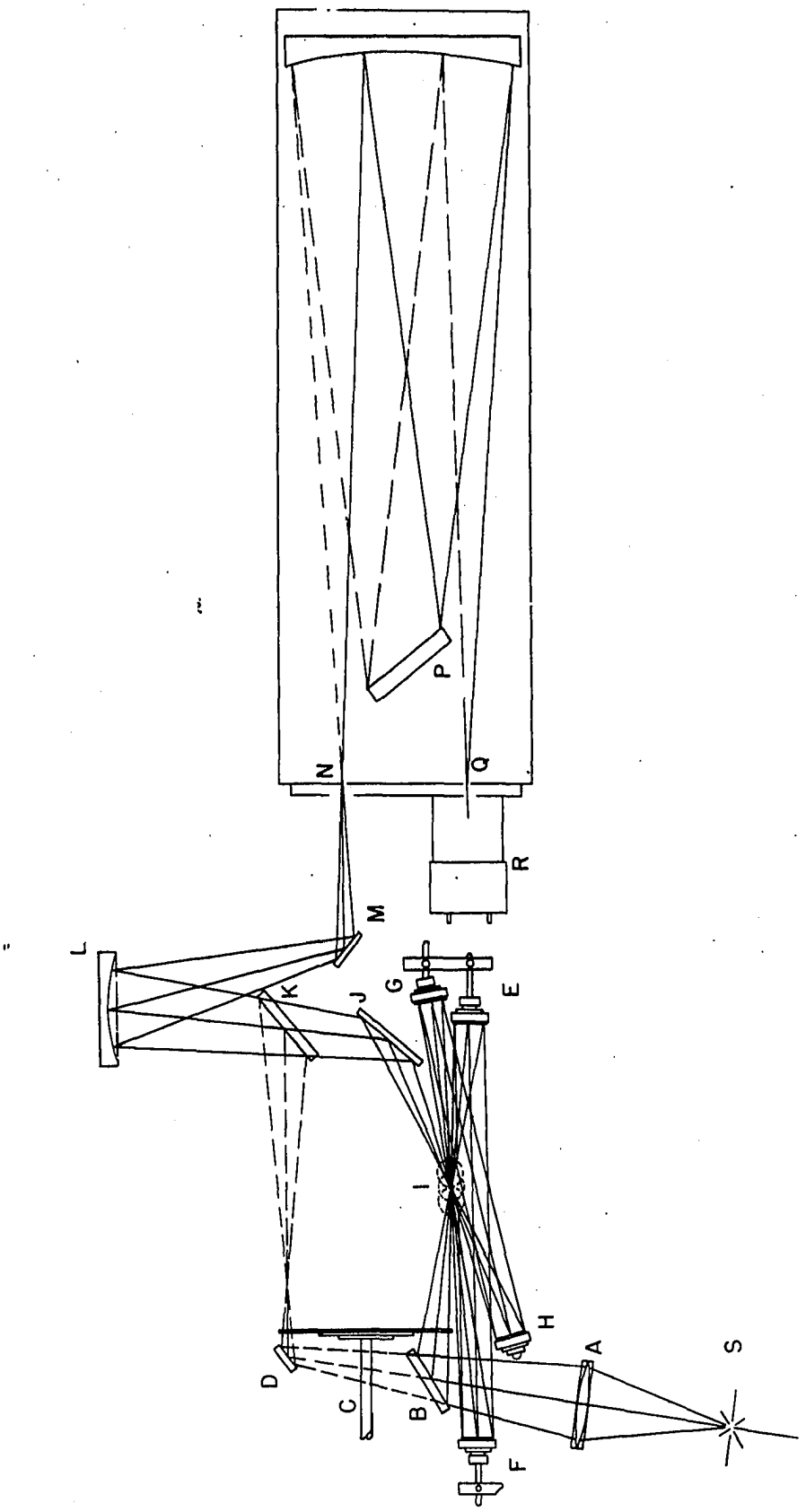
N
Q
P
R
M
L
K
J
G
E
I
H
D
C
B
A
S
F

Table 6. Optical specifications and legend for Figure 10

Identification		Focal length (cm)	Diameter (cm)	Description
A	Lens	13.2	9.5	Double-convex, pyrex
B	Mirror	∞		Front surface
C	Chopper		18	
D	Mirror	∞		Front surface
E	Mirror	10	3	Back surface, quartz
F	Mirror	5	3	Back surface, quartz
G	Mirror	10	3	Back surface, quartz
H	Mirror	10	3	Back surface, quartz
I	Three flames			
J	Mirror	∞		Front surface
K	Mirror	∞		Front surface
L	Mirror	5	8	Front surface
M	Mirror	∞		Front surface
N	Monochromator entrance slit			15 micron
O	Monochromator collimator			f:9
P	Grating	∞		30,000 lines/inch
Q	Monochromator exit slit			15 micron
R	Detector			RCA 1P28

central flame. The multipass optics functioned very much like the system previously described for photographic detection. The remaining energy was passed over mirror B to mirror D which directed the beam through the plane of the 13 cps chopper and then on to the beam-recombining optics. The chopped beams, after passing through the beam-recombining optics, arrived at the entrance slit of the monochromator ninety degrees out of phase. A 0.5 meter Ebert scanning monochromator (Jarrell-Ash #82000) was used to isolate the narrow wavelength region (absorption line) line from the continuous background. The specifications of the monochromator are given in Table 7.

When the single-beam mode of operation was employed, mirror B was replaced by a special full-aperture mirror, and mirror K was removed. In this way all of the energy was directed through the sample channel. This system sampled a seven millimeter high portion of the flame.

4. Detector

An RCA 1P28 photomultiplier tube was used to detect the spectral radiation. This tube is a side-on viewing type with a one inch diameter cathode. The photocathode surface is of the SbCs-type with an over-all S-5 response. The 1P28 has a

Table 7. Characteristics of Jarrell-Ash #82000 Ebert scanning monochromator

Characteristic	Specifications
Optical arrangement	0.5 meter Ebert grating mount arranged as described by Fastie (97). Aperture f:9.
Grating	Plane, replica grating having a ruled area of 27 cm^2; 30,000 lines/inch blazed for 7500 Å.
Slits	Fixed, bayonetting entrance and exit slits. Matched pairs having widths of 0.015 mm were used.
Dispersion and resolution	Reciprocal linear dispersion at exit slit is 16 Å/mm, first order. Resolution is at least 0.2 Å, first order using 0.010 mm slits.
Scanning action	Eight automatic scanning speeds are available. These are 500, 250, 125, 50, 20, 10, 5, and 2 Å/min. Manual scanning is possible. Accuracy of wavelength counter is 2 Å with reproducibility of 0.5 Å.

useful working range between 2000 and 6000 Å with its maximal response at 3400 Å. The nine stages of amplification provide an over-all luminous sensitivity of 50 ampere/lumen with a maximal equivalent dark current of 1.25×10^{-9} lumen. No improvement was found in the absorption signal/noise ratio with an EMI 6255B photomultiplier tube.

5. Electronic system

A Furst Electronics model 710-PR power supply provided the dynode voltage for the photomultiplier tube. This power supply was capable of supplying any voltage from 100 to 1500 volts at currents from 0 to 10 ma. The stability of the power supply was such that no discernible drift was noticed in the voltage output over an extended period of use.

The output of the photomultiplier tube was coupled directly to the 13-cps amplifier, by-passing the transformer coupled preamplifier that was used with thermocouple detection. The tuned amplifier consists of standard dual-triode amplifier circuits and a suitable output stage to match the rectifiers, filters, and load. The gain of the amplifier was sufficiently high that the output signal, after demodulation, could drive a ten millivolt potentiometer recorder. The output was coupled to the mechanical rectifiers by a

transformer.

The breaker-assembly, actuated by the mechanical chopper shaft, consists of three cam-operated, full-wave rectifier sections for separating and rectifying the 13 cps sample and reference signals, and for modulating test signals.

The demodulated signals, after passing through a response filter network, were fed into a Leeds and Northrup Speedomax Type G recorder. A standard 450-ohm resistance slide wire was used, and the original amplifier and damping circuits were retained. The chart speed was set at 1.2 inches per minute.

The details of the Model-13 electronics, including circuit schematics and wiring diagrams, are available through the manufacturer.

The instrument described above provided an accuracy of 0.5 percent in transmittance measurements with an instantaneous reproducibility of 0.5 percent.

6. Burners

In contrast with the results obtained with the 60 cps system of Perkin-Elmer Model-214, three conventional oxygen-acetylene diffusion flames when used with the 13 cps system introduced less than one percent of high frequency noise into

the energy signal. Furthermore, the multipass system was more efficient with the extended diffusion flames than with the premixed flames of smaller diameter described earlier. Therefore, the atomic absorption measurements reported in the remainder of this thesis were made on the fuel-rich oxygen-acetylene diffusion flame of a conventional Beckman burner.

C. Results

1. Recording of absorption spectra

Since the distribution of radiant energy from a high pressure xenon arc is continuous over the ultraviolet and visible regions, it was possible to scan the spectrum for absorption lines. In actual practice, an upper limit was placed on the scan speed by the over-all response of the instrument. Since atomic absorption lines are so narrow, a scan rate greater than ten angstroms per minute in the first order resulted in a loss of sensitivity. An alternative to scanning the absorption lines would have been to set the monochromator on the absorption line and to measure the transmittance of the flame when fed with sample solution and pure solvent alternately. However, possible differences in

the rates of aspiration between the pure solvent and solution could cause significant differences in the light scattering properties and physical geometry of the flames. Hence, for the experiments reported in this section, second order absorption lines were scanned at 2.5 angstroms per minute.

Atomic absorption tracings were made at different concentrations for twenty-six elements including the lanthanides and a number of more common elements. From these spectra it was possible to calculate analytical curves and to determine sensitivities and detection limits. The experimental conditions under which the absorption spectra were recorded are summarized in Table 8. The high stability of the radiant output of the d.c. xenon arc made it possible to use the direct mode of operation throughout these experiments. Since the energy in the sample signal is approximately four times greater with the direct mode, the lower amplifier gain can result in an increase in signal/noise ratio. Tracings of the most sensitive absorption lines of ytterbium, europium, and dysprosium are shown in Figures 11, 12, and 13 respectively. Measurements were made on flames fed with solutions of different concentrations of the metal.

The preparations of the rare earth solutions were

Table 8. Experimental conditions for recording of atomic absorption spectra

Mode of operation	Direct
Photomultiplier voltage	800 volts
Amplifier gain	Determined by wavelength region and extent of scale expansion
Scale expansion	The scale was calibrated with neutral density filters prior to each scan
Time constant	0.6 second
Scan speed	2.5 Å/min
Chart speed	1.25 inch/min
Slit widths	Entrance: 0.015 mm Exit: 0.015 mm
Order	Second for wavelengths below 4300 Å
Gas flow rates	Oxygen: 2.68 l/min/burner Acetylene: 3.16 l/min/burner
Average sample aspiration rates	0.75 ml/min/burner
Solution concentration	Scans were made at various concentrations

Figure 11. Absorption tracings for ytterbium

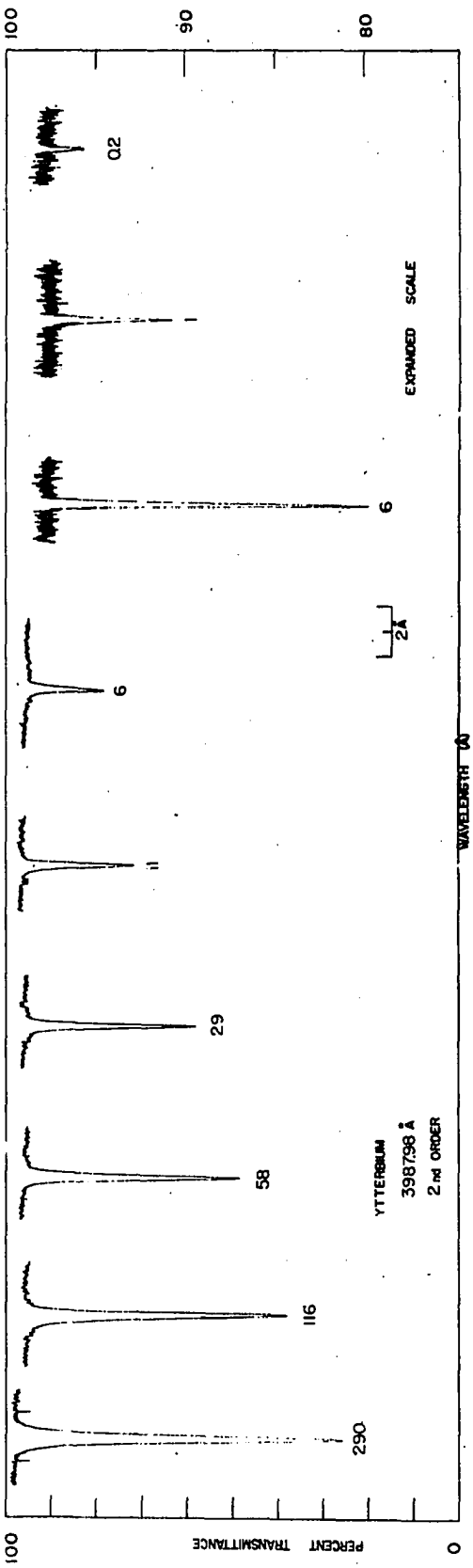
100
90
80
02
EXPANDED SCALE
6
2A
6
11
29
58
116
290
YTTERBIUM
398.798 Å
2nd ORDER
WAVELENGTH
100
PERCENT TRANSMITTANCE
0

Figure 12. Absorption tracings for europium

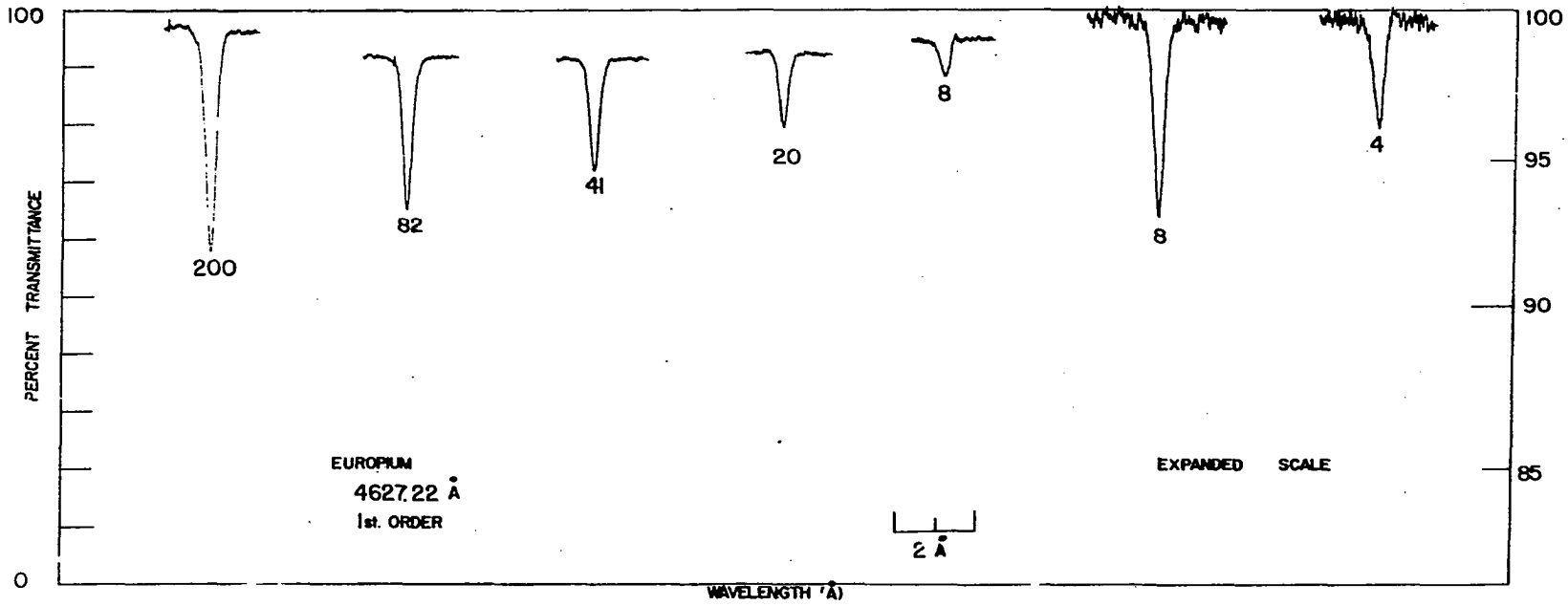
100
0
PERCENT TRANSMITTANCE
200
82
41
20
8
8
4
100
95
90
85
EUROPIUM
4627.22 Å
1st. ORDER
2 Å
EXPANDED SCALE
WAVELENGTH (Å)

Figure 13. Absorption tracings for dysprosium

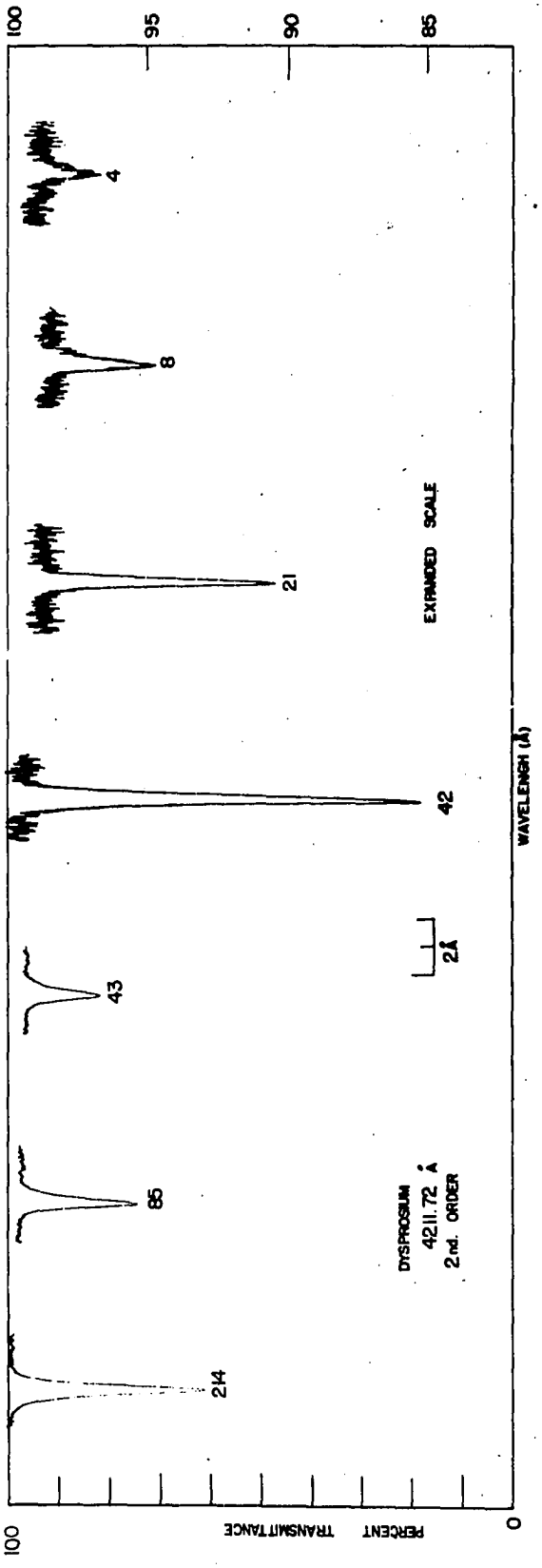
100
95
90
85
4
8
21
EXPANDED SCALE
42
WAVELENGH (Å)
2Å
43
85
214
DYSPROSIUM
4211.72 Å
2nd. ORDER
100
PERCENT TRANSMITTANCE
0

mentioned earlier. Solutions of the common elements were prepared from assayed reagents in accordance with standard techniques. Absolute ethanol was the solvent used for all solutions.

2. Analytical curves

If it is assumed that the shape of the absorption line is due entirely to Doppler broadening and that the spectral band pass of the monochromator is narrow enough to isolate only the center of the absorption line, there will be a linear relationship between the absorption measurement and the concentration (98, p. 100). Unfortunately, the flame environment can contribute to the non-Doppler contour of the absorption lines through pressure broadening and resonance broadening. The latter process will be more important at high concentration of the metal in the flame. Therefore, the flame, in part, contributes to the shape of the working curve, making a different contribution for different elements. Furthermore, the instrumental technique described above does not give an exact measurement of the maximal absorption coefficient. An exact measurement would require a monochromator of much higher dispersion. Hence, the shape of the analytical curve is determined to a certain extent by the

instrumental arrangement used.

Analytical curves are shown in Figures 14-18 for those lanthanides most sensitive in absorption. Marked departure from a non-linear relationship between the absorbance and concentration is apparent in several of the figures. This behavior is not unique to analyses with a continuous source. Quite the contrary, curvature in the analytical curve seems to be the rule rather than the exception with methods employing a line source for absorption measurements.

3. Detection limits

The analytical sensitivity has been defined as that concentration of element that produces an absorption of one percent (95, 99). So defined, analytical sensitivity is a useful measure for comparing atomic absorption procedures and equipment; it does not necessarily reflect the actual detection limit. A realistic detection limit is defined as the concentration that produces an absorption equivalent to twice the standard deviation of the recorded noise level. The concept of detection limit is more useful because it includes not only the factors which govern analytical sensitivity but also the factors which control the noise level.

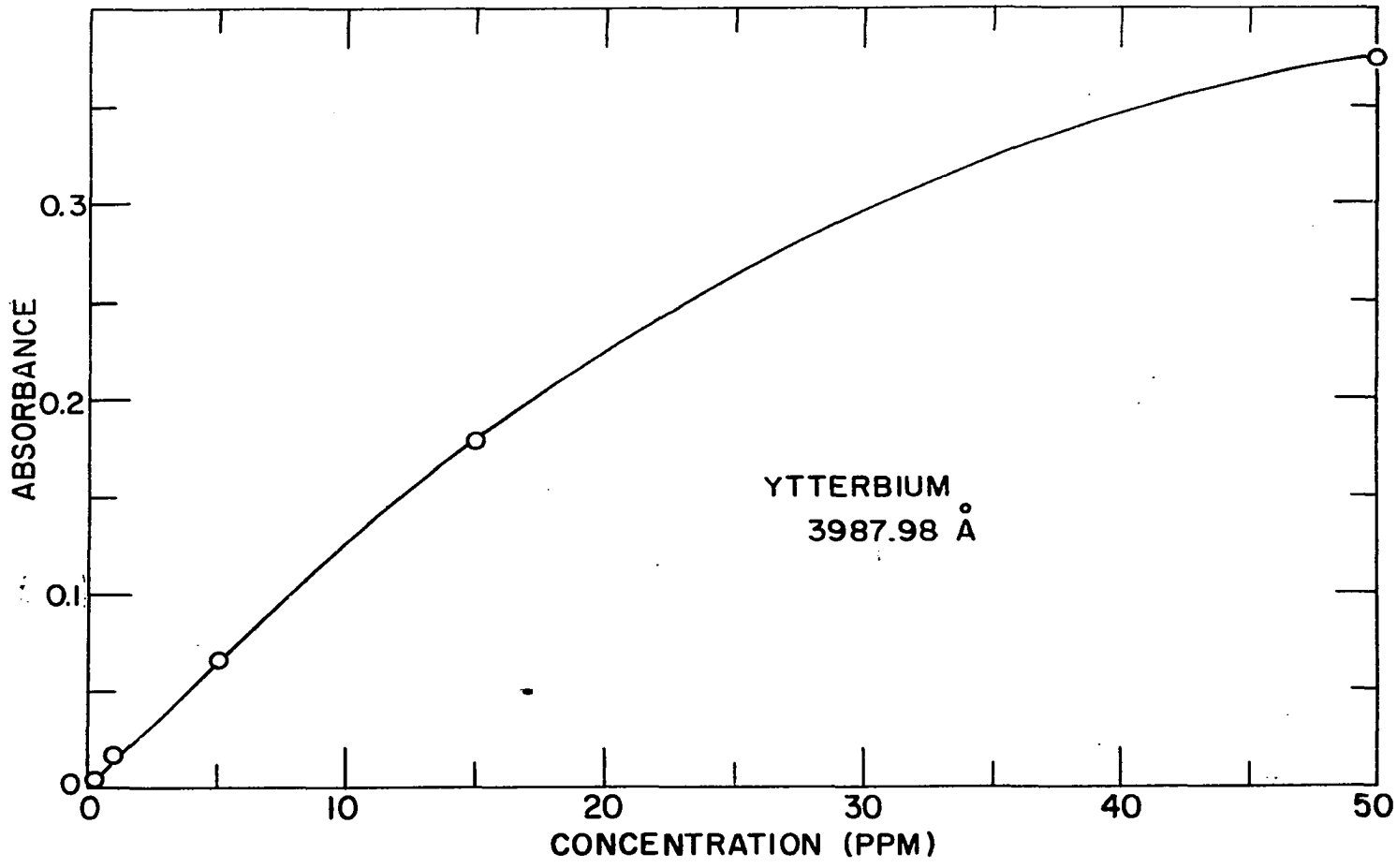

Figure 14. Curve for ytterbium

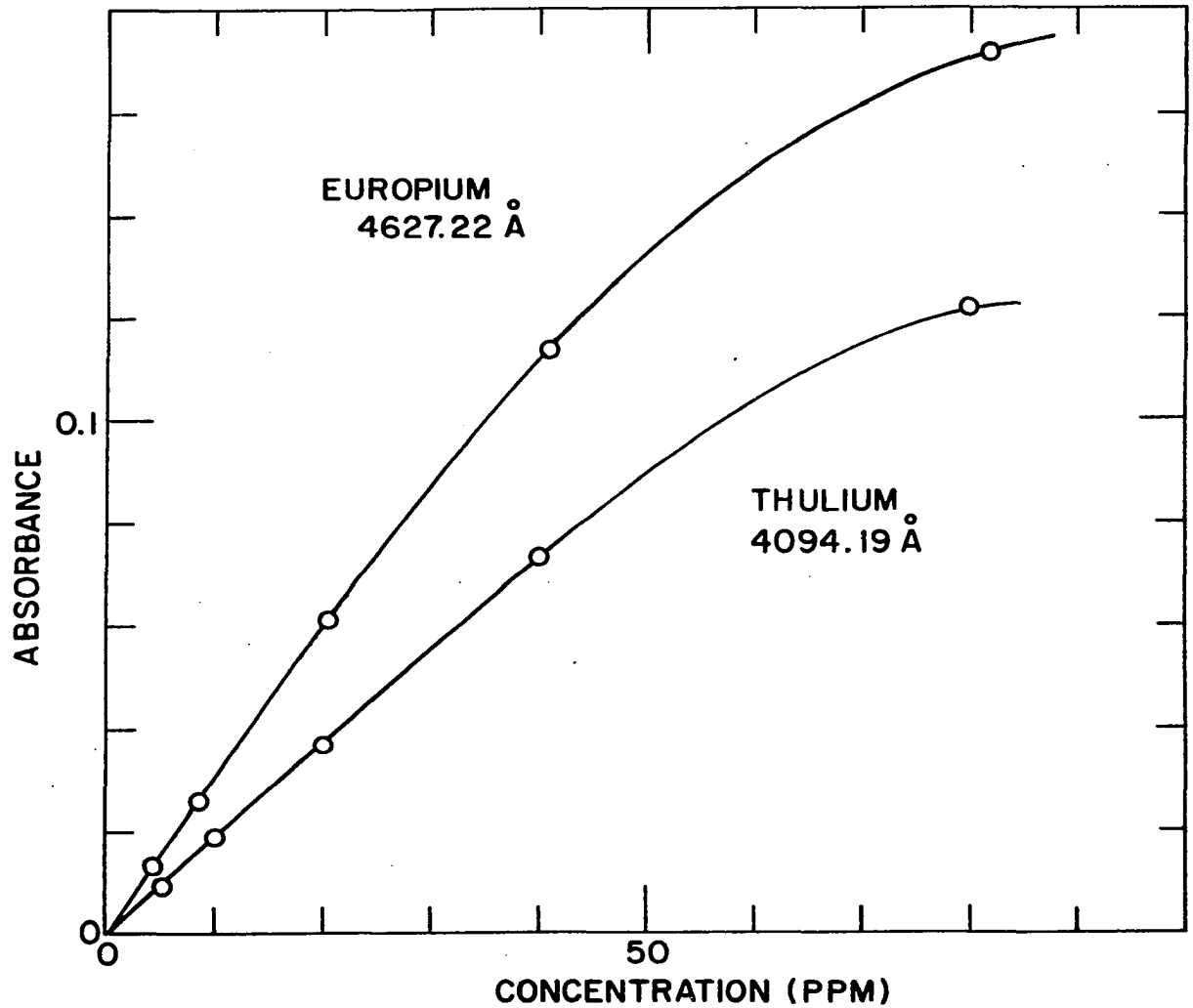

Figure 15. Curve for europium and thulium

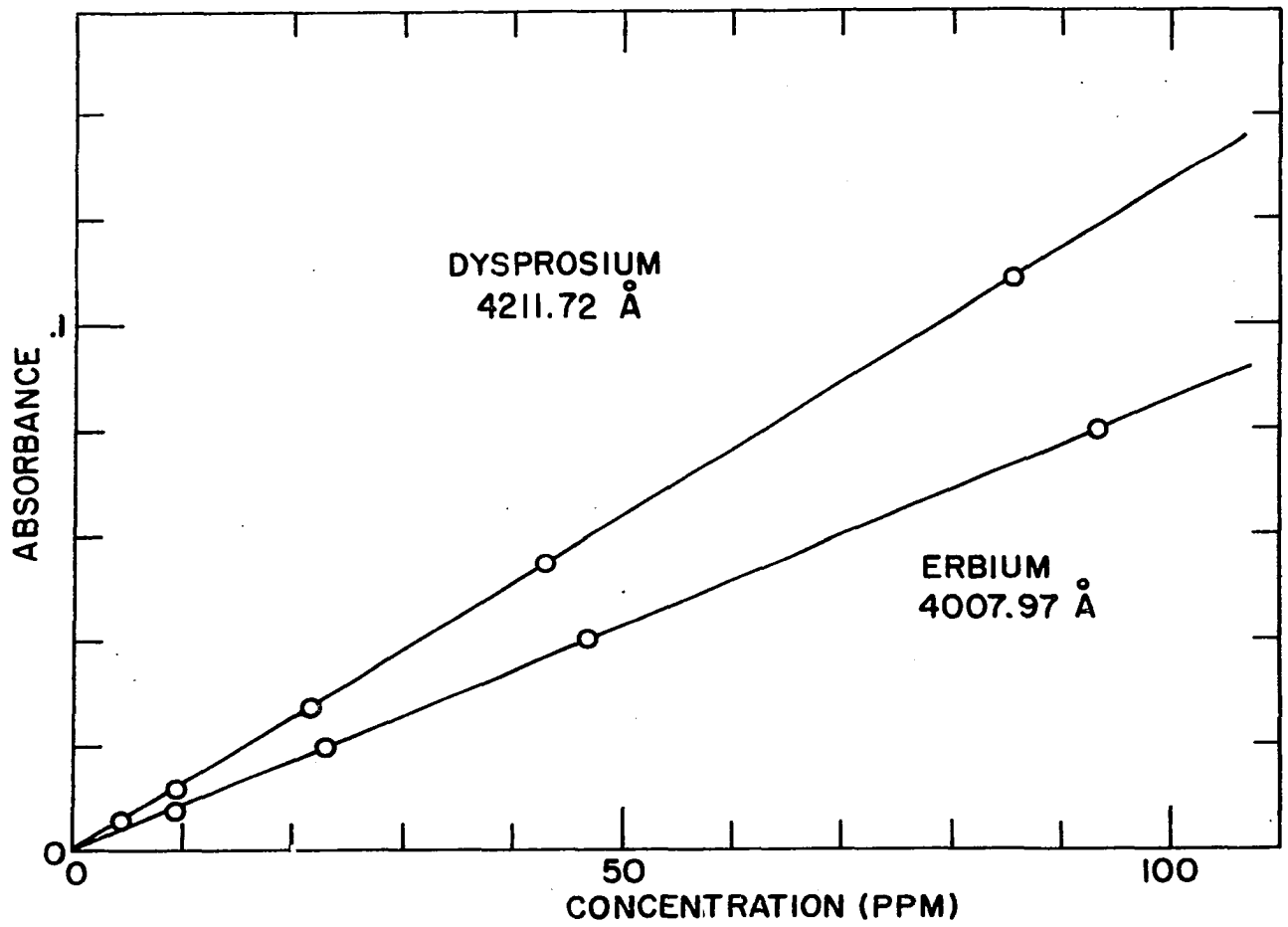

Figure 16. Curve for dysprosium and erbium

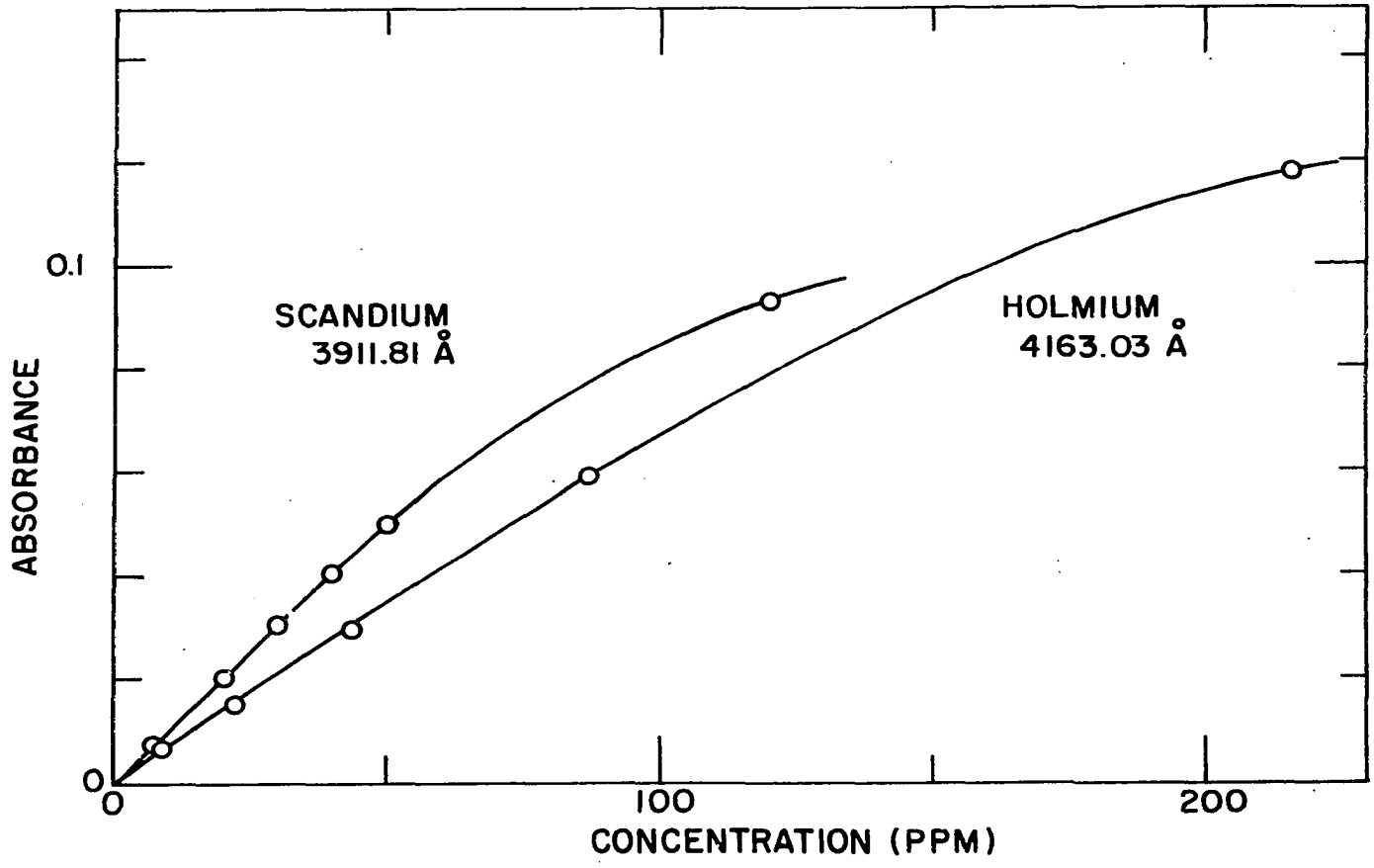

Figure 17. Curve for scandium and holmium

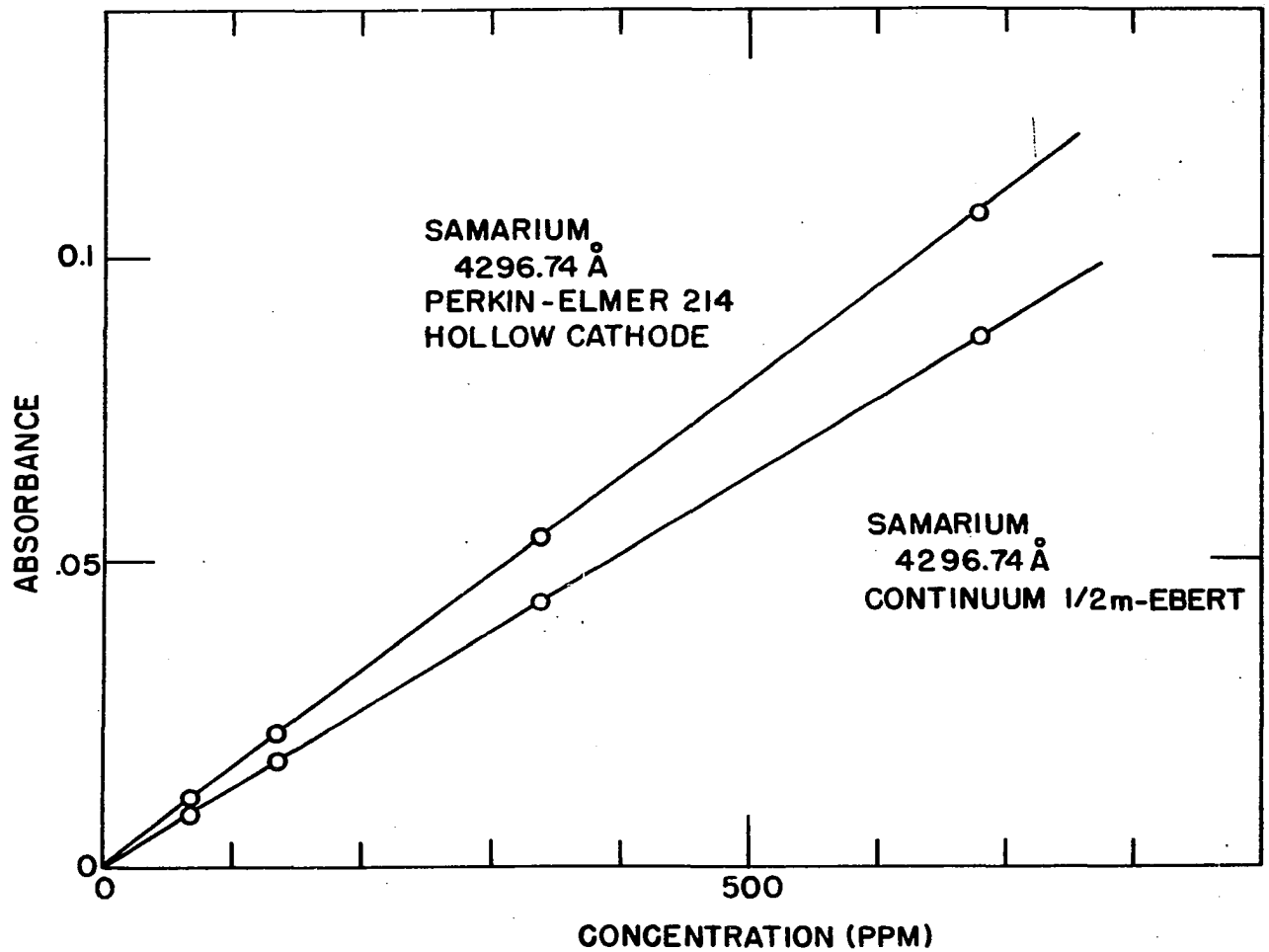

Figure 18. Curves for samarium

Analytical detection limits of twenty-eight elements were determined with the Model-13 and are listed in Table 9. Included are the lanthanides and a number of common metals. Also tabulated in Table 9 are the best values for the detection limits of the elements as reported in the literature. In all cases the values quoted in the literature were obtained with a line source.

Skogerboe and Woodriff (100, 101), using fuel-rich oxygen-acetylene flames, have recently reported sensitivities for six of the rare earth elements. It is worth noting that these workers used an oxygen-hydrogen flame for the emission source in the work done on ytterbium, thulium, and europium.

For several of the elements studied, the best absorption lines were in the spectral range below the Pyrex cutoff at 3200 Å. Allan (102) reports the cobalt 2407 Å line to be fifty times as sensitive as the 3527 Å line in absorption and the nickel 2320 Å line to be fifteen times as sensitive as the 3415 line in absorption. These factors, when applied to the detection limits obtained with a continuum, give values that compare favorably with those obtained with hollow-cathode lamps. This seems to be true in all cases where legitimate comparisons can be made. For manganese and iron

the best lines are reported to be 2795 and 2483 Å respectively, again below the Pyrex cutoff (103). In the cases of silver and copper, the comparison is not entirely fair because the radiant energy emitted by the source at 3200 Å was attenuated to less than ten percent by the Pyrex lens. Here, the signal/noise ratio was somewhat lower. This situation can be improved if the Pyrex source-lens is replaced with a mirror or with a quartz lens.

It is interesting to note that without exception the detection limits reported by Slaven and Manning (104) are substantially lower than those reported by other workers. This no doubt reflects the much lower noise levels attainable with the new Perkin-Elmer Model-303 atomic absorption spectrophotometer.

Analytical sensitivities attainable with a spectral continuum can be unfavorably influenced by the continuous distribution of ghost-radiation arising from periodic spacing errors in the rulings on the diffraction grating. The intensity of a given ghost order rises as the square of the spectral order; therefore, the ghost-spectrum could become a serious problem when a grating of poor quality is used in the second or third order with a spectral continuum. This prob-

Table 9. Detection limits of various metals by atomic absorption spectroscopy

Metal	Wavelength (Å)	Xenon arc source		Detn. limits quoted in literature
		Sensitivity (ppm/abs)	Detection[a] limit (ppm)	Skogerboe (100)[b]
Lanthanum	3574.43	undetected at 10,000		
Cerium[c]		undetected at 10,000		
Praseodymium	4951.36[d]	620	310	
Neodymium	4924.43[d]	105	110	
Samarium	4296.74	44	44	40
Europium	4594.03			12[e]
	4627.22[d]	2.2	1.1	15[e]

[a]The author defined the detection limit to be the concentration of the metal in solution that produced an absorption equivalent to twice the standard deviation of the recorded noise level on either side of the absorption line.

[b]Skogerboe calculated detection limits on the basis of five percent absorption; this figure represented approximately 0.9 of the peak-to-peak noise (100).

[c]Cerium lines were undetected with the photographic technique.

[d]These lines were scanned in the first order.

[e]Oxygen-hydrogen flames were used as the line source for these elements (101).

Table 9 (Continued)

Metal	Wavelength (Å)	Xenon arc source		Detn. limits quoted in literature
		Sensitivity (ppm/abs)	Detection[a] limit (ppm)	Skogerboe (100)[b]
Gadolinium	4078.70	355	360	
Terbium	4326.47	102	133	
Dysprosium	4211.72	2.2	1.1	5.3
Holmium	4163.03	7.3	7.3	5.0
Erbium	4007.97	6.4	1.9	3.0
Thulium	4094.19	2.7	1.9	3.5[e]
Ytterbium	3987.98	0.27	0.32	10[e]
Scandium	3911.81	5.5	2.15	
Yttrium	4077.38	57	57	

Table 9 (Continued)

Metal	Wavelength (Å)	Xenon arc source		Detn. limits quoted in literature		
		Sensitivity (ppm/abs)	Detection[a] limit (ppm)	Slavin[f] (104)	Gatehouse[g] & Willis (99)	Robinson (105)[h]
Neodymium	4058.94	100	100	undetected		
Titanium	3653.50	32	37	15[i]		
	4981.73			undetected		
Rhenium	3460.46	16	17			
	3464.73	16	17			

[f]Slavin's figures are for the detection limit defined as the concentration that produces an absorption equivalent to twice the magnitude of the fluctuation in the background (zero absorption). Fluctuations are reported to be on the order of 5 parts in ten thousand of the total signal. In most cases, an air-acetylene flame was used. The exceptions are designated.

[g]Gatehouse and Willis define the detection limit as the concentration of metal which gave one percent absorption; in several cases, the noise level was lower. A ten centimeter air-acetylene flame was used to produce the atomic vapor.

[h]The limit of detection defined by Robinson was that concentration that gave an absorption equivalent to 2/3 of the noise level of the hollow-cathode signal.

[i]An oxygen-acetylene flame was required to produce the atomic vapor (106).

Table 9 (Continued)

Metal	Wavelength (Å)	Xenon arc source: Sensitivity (ppm/abs)	Xenon arc source: Detection[a] limit (ppm)	Detn. limits quoted in literature: Slavin[f] (104)	Detn. limits quoted in literature: Gatehouse[g] & Willis (99)	Detn. limits quoted in literature: Robinson (105)[h]
Vanadium	3183.98			9[i]	undetected	300[j]
	4379.24	53	63	127[i]		
Chromium	3578.69	0.29	0.31	0.01	0.15	0.05[k]
Manganese	2794.82			0.01	0.05	
	4030.76	3.1	4			
Iron	2483.27			0.05	0.1	
	3719.94	4.5	5.3		1	4[k]
Cobalt	2407.25			0.15	0.2	
	3526.85	8.5	8.5		4	10[k]
Nickel	2320.03			0.05	0.2	
	3414.76	4.4	4.4		0.5	0.5[j]
	3524.54	4.4	4.4			0.5[j]

[j]An oxygen-acanogen flame was used to produce the atomic vapor.

[k]An oxygen-hydrogen flame was used to produce the atomic vapor.

Table 9 (Continued)

Metal	Wavelength (Å)	Xenon arc source		Detn. limits quoted in literature		
		Sensitivity (ppm/abs)	Detection[a] limit (ppm)	Slavin[f] (104)	Gatehouse[g] & Willis (99)	Robinson (105)[h]
Copper	3247.57			0.005	0.1	0.2[j]
	3273.96	2.8	11			
Silver	3280.68	8.7	1.8	0.02	0.05	0.2[j]
Calcium	4226.73	0.067	0.060	0.01	0.08	
Sodium	5889.95	0.057	0.050		0.03	0.5[j]

lem does not apply to atomic absorption techniques in which a line source is used since it is unlikely that a ghost-line will be exactly superimposed upon an absorption line at the exit slit of the monochromator.

D. Conclusion

It is evident from the data in Table 9 and from the absorbance versus concentration curves that the atomic absorption spectra of at least seven of the lanthanide elements are analytically useful. Certainly, these observations extend the practical range of application of atomic absorption spectroscopy.

The investigation of the rare earth absorption spectra has disclosed some rather remarkable facts concerning the use of a 150-watt xenon compact arc lamp as a source for atomic absorption. (a) The energy emitted over a 0.12 Å spectral slit-width is more than enough to give a satisfactory signal/noise ratio for a very large region of the visible-ultraviolet spectrum. The limits to which the xenon arc can be extended still have not been determined. (b) Many atomic absorption lines can be isolated from a continuous background with a table-model monochromator having a spectral band pass

of 0.12 Å. The economy minded spectroscopist will find this very interesting. (c) The radiant output of the d.c. xenon compact arc is of such stability that dual-beam optics for source monitoring are unnecessary and an added expense. (d) The analytical detection limits obtainable with a continuous source used in conjunction with a table-model monochromator and photoelectric detection compare quite favorably with those obtainable with line sources. Besides the economic advantage provided by the use of one source to analyze for many elements, considerable gain in time is achieved by circumventing the realignment procedure. This factor alone could help put atomic absorption analysis on a more routine basis. The promising results described in this section suggest that atomic absorption will emerge as a complementary technique to emission flame photometry.

E. Suggestions for Further Investigation

The findings reported in the foregoing section open the way into many avenues of exploration in the young field of analytical atomic absorption spectroscopy. Firstly, it would be interesting to determine whether the analytical sensitivities attainable with a continuous light source can be

significantly improved when high dispersion equipment is employed. The high dispersion direct reading spectrographs available in many laboratories readily could be adaptable to atomic absorption. This is especially true since dual-beam optics are unnecessary. (Such a study has been undertaken by the author. Unfortunately, because the results are incomplete they have not been included in this thesis. There is still a great deal of work that remains to be done.)

Secondly, if the continuum is to be fully exploited as a spectroscopic light source for atomic absorption, observations should be extended into the 2000-3000 Å region. Here, analytical atomic absorption will supersede emission flame photometry by far. Steps also have been taken in this direction, but further work is necessary.

Chemical interferences resulting in inefficient sample atomization by the flame system used probably are the major obstacles to the continued development of atomic absorption as an analytical method. As mentioned earlier, workers are seeking other systems as the means of reducing a sample to the atomic state. One candidate that merits investigation is the plasma jet.

Because a large number of elements were studied and

adequate instrumentation had to be developed, the investigation of the atomic absorption spectra of the rare earths was restricted to general observations. It would be valuable, now, to focus attention on the rare earths as individual elements rather than as a group. Assessment of cross-interferences of the lanthanides in complex mixture determinations would be worthwhile.

V. SUMMARY

Heretofore, the atomic absorption flame spectra of some twenty-eight elements including the rare earths have not been reported in the literature. The basic problem presented by this group of elements arises from the formation of exceptionally stable molecular species in conventional stoichiometric flames, a situation resulting in the inefficiency of sample atomization. The deficiency in this technique has been partly overcome through the operation of oxygen-acetylene flames under markedly fuel-rich conditions. It has been shown in this thesis that the fuel-rich oxygen-acetylene flame provides a more favorable environment for the existence of free atoms of the elements in this group. Through this expedient more than 1000 rare earth absorption lines have been observed and their wavelengths and relative strengths have been estimated. These wavelengths provide a convenient starting point in the analysis of atomic spectral structure; therefore, they are of significant value.

Inquiry was made into the nature of the flame environment. A reasonable mechanistic scheme was proposed to account for the observed enhancements in atomic emission and

absorption spectra of those elements that have a strong predilection to form stable monoxide molecules in stoichiometric flames. This mechanism was judged in the light of existing data on hydrocarbon flames.

A double-beam atomic absorption spectrophotometer was assembled from the electronic and optical components of an infrared spectrophotometer. This instrument was used to evaluate the analytical potentialities of the atomic absorption spectra of the lanthanide elements and to assess the usefulness of a spectral continuum as a spectroscopic light source for atomic absorption. The continuous source in conjunction with low dispersion and photoelectric detection have furnished analytically useful atomic absorption spectra of many of the lanthanides and a host of common elements. Since many of these elements have evaded detection by flame atomic absorption techniques in which stoichiometric or less fuel-rich flames were used, the observations reported in this thesis should widen the potential scope of application of this promising new technique.

VI. LITERATURE CITED

1. Paul, F. W., Phys. Rev. 49, 156 (1936).

2. Paul, F. W., Phys. Rev. 47, 799 (1935).

3. Bovey, L. F. H. and Garton, W. R. S., Proc. Phys. Soc. (London) 67A, 291 (1954).

4. Bovey, L. F. H. and Garton, W. R. S., Proc. Phys. Soc. (London) 67A, 476 (1954).

5. Sugar, J., J. Research Natl. Bur. Standards 66A, 321 (1962).

6. Worden, E. F., Gutmacher, R. G., and Conway, J. G., Appl. Opt. 2, 707 (1963).

7. Walsh, A., Spectrochim. Acta 7, 108 (1955).

8. Walsh, A., Advances in Spectroscopy 2, 1 (1961).

9. Robinson, J. W., Anal. Chem. 32, 17A (1960).

10. Robinson, J. W., Progress in Nuclear Energy 2 Series 9, 224 (1961).

11. Robinson, J. W., Ind. Chemist 38, 226 (1962).

12. Butler, L. R. P., S. African Ind. Chemist 15, 162 (1961).

13. Polvektov, N. W., Zavodskaya Lab. 27, 830 (1961).

14. Allan, J. E., Spectrochim. Acta 18, 605 (1962).

15. David, D. J., Analyst 85, 779 (1960).

16. Menzies, A. C., Anal. Chem. 32, 898 (1960).

17. Leithe, W., Angew. Chem. 73, 488 (1961).

18. Perkin-Elmer Corporation [Norwalk, Conn.] Atomic Absorption Newsletters 1-8, (1962).

19. Willis, J. B., Methods of Biochemical Analysis 2, 1 (1963).

20. Gilbert, P. T., Jr., Anal. Chem. 34, 210R (1962).

21. David, D. J., Spectrochim. Acta 20, 1185 (1964).

22. Elwell, W. T. and Gidley, J. A. F., Atomic Absorption Spectrophotometry, Oxford, Pergamon Press (1961).

23. Tremmel, C. G., Flame Spectrometric Determination of Lanthanum in Rare Earth Mixtures. Unpublished M.S. thesis. Ames, Iowa, Library, Iowa State University of Science and Technology. (1958).

24. Fassel, V. A., Curry, R. H., and Kniseley, R. N., Spectrochim. Acta 18, 1127 (1962).

25. Fassel, V. A. and Mossotti, V. G., Anal. Chem. 35, 252 (1963).

26. Gatehouse, B. M., Sullivan, J. V., and Walsh, A., Nature 192, 929 (1961).

27. Goleb, A. and Brody, J. K., Applied Spectroscopy 16, 47 (1962).

28. Gatehouse, B. M. and Walsh, A., Spectrochim. Acta 16, 602 (1960).

29. Walsh, A., Proc. Colloq. Spectroscopicum Intern., 1962, 10th, 127 (1963).

30. Robinson, J. W., Anal. Chim. Acta 27, 465 (1962).

31. L'vov, B. V., Spectrochim. Acta 17, 761 (1961).

32. Bochkova, O. P. and Schreider, E. Ya., Izvest. Akad. Nauk S.S.S.R. Ser. Fiz. 19, 75 (1955). Original not available; abstracted in C.A. 50:3887e.

33. Nelson, L. S. and Kuebler, N. A., Spectrochim. Acta 19, 781 (1963).

34. Carlson, F. E., J. Soc. Motion Picture Engrs. 48, 395 (1947).

35. Aldington, J. N. and Meadowcroft, A. J., J. Inst. Elec. Engrs. (London) 5, 671 (1948).

36. Meadowcroft, A. J., Phot. J. 89B, 51 (1949).

37. Robinson, J. W. and Harris, R. J., Anal. Chim. Acta 26, 439 (1962).

38. Bulewicz, E. M. and Sugden, T. M., Trans. Faraday Soc. 54, 830 (1958).

39. Feldman, C. and Ellenburg, J. Y., Spectrochim. Acta 7, 349 (1956).

40. Fassel, V. A., Myers, R. B., and Kniseley, R. N., Spectrochim. Acta 19, 1187 (1962).

41. Harrison, G. R., ed., Massachusetts Institute of Technology Wavelength Tables, New York, N. Y., John Wiley (1939).

42. Meggers, W. F., Corliss, C. H., and Scribner, B. F., National Bureau of Standards Monograph 32, Part 1, 1 (1961).

43. Mossotti, V. G. and Fassel, V. A., Spectrochim. Acta 20, 1117 (1963).

44. Curry, R. H., Flame Spectroscopy of the Rare Earth Elements. Unpublished Ph.D. thesis. Ames, Iowa, Library, Iowa State University of Science and Technology. (1962).

45. Grossman, W. E. L., Some Physico-Chemical Considerations in Flame Spectroscopy. Unpublished Ph.D. thesis. Ithaca, New York, Library, Cornell University. (1964).

46. Broida, H. P. and Heath, D. F., J. Chem. Phys. 26, 223 (1957).

47. Fenimore, C. P. and Jones, G. W., J. Phys. Chem. 62,

178 (1958).

48. Alkemade, C. Th. J., Proc. Colloq. Spectroscopicum Intern., 1962, 10th, 143 (1963).

49. Sugden, T. M., Ann. Rev. Phys. Chem. 13, 369 (1962).

50. Mavrodineanu, R., Spectrochim. Acta 17, 1016 (1961).

51. Broida, H. P. and Shuler, K. E., J. Chem. Phys. 27, 933 (1957).

52. Gilbert, P. T., Jr., Proc. Colloq. Spectroscopicum Intern., 1962, 10th, 171 (1963).

53. Calcote, H. F., Symp. Combust., 1960, 8th, 184 (1962).

54. De Jaegere, S., Deckers, J., and Van Tiggelen, A., Symp. Combust., 1960, 8th, 155 (1962).

55. Mukherjee, N. R., Fueno, T., Eyring, H., and Ree, T., Symp. Combust., 1960, 8th, 1 (1962).

56. Van Tiggelen, A., Bertrand, J. N., and Philippaerts, H., U. S. Atomic Energy Commission Report No. AD-258,050 [Armed Services Technical Information Agency, Dayton, Ohio]. (1961).

57. Bascombe, K. N., Green, J. A., and Sugden, T. M., Advances in Mass Spectrometry, Proc. Conf., 1960, 2nd, 66 (1961).

58. Berendsen, R., Taelemans, G., and Van Tiggelen, A., Bull. soc. chim. Belges 69, 32 (1960).

59. Knewstubb, P. F. and Sugden, T. M., Nature 181, 474 (1960).

60. Knewstubb, P. F. and Sugden, T. M., Proc. Roy. Soc. (London) A255, 520 (1960).

61. Deckers, J., Symp. Combust., 1958, 7th, 284 (1959).

62. Feuno, T., Mukherjee, N. R., Ree, T., and Eyring, H., Symp. Combust., 1960, 8th, 222 (1962).

63. Calcote, H. F., Combustion and Flame 1, 385 (1957).

64. Calcote, H. F. and King, R. I., Symp. Combust., 1954, 5th, 423 (1955).

65. Field, F. H. and Franklin, J. L., Electron Impact Phenomena, New York, Academic Press, Inc. (1957).

66. Tal'roze, V. L. and Frankevitch, E. L., J. Am. Chem. Soc. 80, 2344 (1958).

67. Gilbert, P. T., Jr., Am. Soc. Testing Materials Spec. Tech. Publ. 269, 73 (1960).

68. Knewstubb, P. F. and Sugden, T. M., Research Correspondence 9, A1 (1956).

69. Padley, P. J. and Sugden, T. M., Symp. Combust., 1960, 8th, 164 (1962).

70. Belcher, H. and Sugden, T. M., Proc. Roy. Soc. (London) A202, 17 (1950).

71. Goldstein, H. W., Walsh, P. N., and White, D., J. Phys. Chem. 65, 1400 (1961).

72. Walsh, P. N., Dever, D. F., and White, D., J. Phys. Chem. 65, 1410 (1961).

73. Walsh, P. N., Goldstein, H. W., and White, D., J. Am. Ceram. Soc. 43, 229 (1960).

74. Herzberg, G. H., Spectra of Diatomic Molecules 2nd ed., Princeton, N. J., D. Van Nostrand Co., Inc. (1950).

75. Calcote, H. F. and Reuter, J. L., Instrument Society of America, Meeting, 1961, Preprint 69-LA-61 (1961).

76. David, D. J., Analyst 83, 655 (1958).

77. David, D. J., Nature 184, 1195 (1959).

78. Willis, J. B., Nature 186, 249 (1960).

79. Willis, J. B., Spectrochim. Acta 16, 259 (1960).

80. Gidley, J. A. F. and Jones, J. T., Analyst 85, 249 (1960).

81. David D. J., Analyst 84, 536 (1959).

82. David, D. J., Analyst 85, 495 (1960).

83. Wallace, F. J., Analyst 88, 259 (1963).

84. Belcher, C. B. and Bray, H. M., Anal. Chim. Acta 26, 322 (1962).

85. Andrew, T. R. and Nichols, P. R. N., Analyst 87, 25 (1962).

86. David, D. J., Analyst 86, 730 (1961).

87. Strasheim, A. and Wessels, G. J., Appl. Spectroscopy 17, 65 (1963).

88. Clinton, O. E., Spectrochim. Acta 16, 985 (1960).

89. Corliss, C. H., Bozman, W. R., and Westfall, F. O., J. Opt. Soc. Amer. 43, 398 (1953).

90. Kniseley, R. N., D'Silva, A. P., and Fassel, V. A., Anal. Chem. 35, 910 (1963).

91. Russell, B. J. and Walsh, A., Spectrochim. Acta 15, 883 (1959).

92. Allan, J. E., Analyst 83, 466 (1958).

93. Dieke, G. and Crosswhite, H. M., J. Opt. Soc. Amer. 42, 433 (1952).

94. Jones, W. G. and Walsh, A., Spectrochim. Acta 16, 249 (1960).

95. Allan, J. E., Spectrochim. Acta 18, 259 (1962).

96. Gibson, J. H., Grossman, W. E. L., and Cooke, W. D., Proc. Feigl Anniversary Symp., Amsterdam, Elsevier Publishing Co. (1962); also abstracted in Appl. Spectroscopy 16, 47 (1962).

97. Fastie, W. G., J. Opt. Soc. Am. 42, 641 (1952).

98. Mitchell, A. C. G. and Zemansky, M. W., Resonance Radiation and Excited Atoms, Cambridge, Cambridge University Press (1961).

99. Gatehouse, B. M. and Willis, J. B., Spectrochim. Acta 17, 710 (1961).

100. Skogerboe, R. K., Study of the Optimum Conditions for the Analysis of Some Rare Earths by Atomic Absorption Methods. Unpublished Ph.D. thesis. Bozeman, Montana, Library, Montana State College. (1963).

101. Skogerboe, R. K. and Woodriff, R. A., Anal. Chem. 35, 1977 (1963).

102. Allan, J. E., Nature 187, 1110 (1960).

103. Allan, J. E., Nature 15, 800 (1959).

104. Perkin-Elmer Corporation [Norwalk, Conn.] Atomic Absorption Newsletter 18, (1964).

105. Robinson, J. W., Anal. Chem. 33, 1067 (1961).

106. Slavin, W. and Manning, D. C., Anal. Chem. 35, 253 (1963).

VII. ACKNOWLEDGEMENTS

The author considers it a privilege to have worked under Dr. Velmer A. Fassel and wishes to thank him for the inspiration, stimulation, and interest which were freely given throughout the course of this investigation. The acceptance of the author into his spectrochemistry group after previous graduate study is particularly appreciated.

The skill and helpfulness of Dr. William E. L. Grossman were of great value in the completion of this research. The author also wishes to extend sincere appreciation to Mr. Richard N. Kniseley for the many beneficial discussions during the course of this investigation.

The author is indebted to Mr. Danold W. Golightly for his assistance in photographing the spectra and in constructing the equipment; also, the able technical assistance of Mr. William B. Barnett and Mrs. Otto W. Maender is greatly appreciated.

Lastly, the author is grateful to his wife, Cecil May, for her assistance in the preparation of this manuscript.